Tectonics of the Georgia Basin, northwest Washington State, USA, and southwest British Columbia, Canada

Peter Michael Polivka

A thesis submitted in partial fulfillment of the requirements for the degree of

Master of Science

University of Washington
2013

Committee:
Thomas L. Pratt
Joseph Wartman
Kathy Troost

Program Authorized to Offer Degree: Civil & Environmental Engineering

University of Washington

Abstract

Tectonics of the Georgia Basin, northwest Washington State, USA, and southwest British Columbia, Canada

Peter Michael Polivka

Chair of the Supervisory Committee:
Affiliate Professor Dr. Thomas L. Pratt
Department of Earth & Space Sciences / School of Oceanography

GPS strain and recent neotectonic studies in northwest Washington and southwest British Columbia indicate long term north-south shortening of the Cascadia forearc extends north of recognized active faults. This study reviews seismic reflection profiles from the SHIPS 1998 and 2002 experiments in conjunction with industry data to identify active geologic structures capable of accommodating this unaccounted strain. Here a new active northeast striking thrust system in southern Strait of Georgia is identified, the fault ruptured during the 1997 earthquake near Gabriola Island and Vancouver B.C. is imaged, and the first subsurface images of the Sandy Point Fault are presented.

TABLE OF CONTENTS

ACKNOWLEDGEMENTS

Michael Riedel for making the 2002 SHIPS data available and playing host at the Pacific Geoscience Center of the Geological Survey of Canada. John Cassidy, Roy Hyndman, and many more at the Pacific Geoscience Center provided new perspectives and encouragement. Brian Sherrod and Harvey Kelsey for continuous bantering, and occasional discussions, about the study area. Richard Blakely for help and insight on gravity and magnetic data. Aaron Fircke and Rip Hale for discussions on sediment waves. Ralph Haugerud for discussions on geology along the US-Canadian Border. Robert Bernis for providing the Haxby colorblind earth sciences colormap freely via the MatLab File Exchange. Focal mechanisms are plotted with GMT by the generous work of Paul Wessel, Walter H. F. Smith, and their team at the University of Hawaii. This work would not have been possible without the collective effort of the crews aboard the R/V Thompson and R/V Tully during the 1998 and 2002 SHIPS cruises. William Wilcock for encouragement, guidance, and assistance at unreasonable hours. Lastly, Trudy Cervantes, for making miracles happen.

DEDICATION

To my parents and their unwavering support.

Chapter 1. INTRODUCTION

The Strait of Georgia of southwest Canada and the northwest U.S. mainland is an inland waterway that occupies the forearc basin of the northern Cascadia subduction zone (figure 1). The Strait of Georgia stretches more than 200 km north between mainland Canada and Vancouver Island, from the U.S./Canadian border in the southeast to central Vancouver Island in the northwest. The topographic low underlying the Strait of Georgia has had multiple models proposed for its formation, one being Cretaceous to Eocene margin-parallel strike-slip motion (Johnson, 1985). Basin formation has recently been recognized to have resulted from syndepositional thrusting along both sides of the basin, shifting the model from that of a forearc basin to that of a foreland basin (Mustard, 1994).

A thick sedimentary sequence composed of marine Cretaceous and non-marine Eocene strata underlies the strait and is exposed along its edges (figure 2). Cretaceous shale beds have been explored for fossil fuels since the first Strait of Georgia settlers in the mid-1800s. Coal for household heating was the original prize spurring geologic exploration. Localized tar seeps, inferred to originate from volatilization of coal beds by intrusive igneous events (Bell, 1967), led to several "off-shore" and onshore hydrocarbon surveys in the region. Despite perceived reserves (Bell, 1967) large-scale production never occurred, presumably because of small volumes, poor capping, or both. A limited amount of data from these commercial surveys has been published (England and Calon, 1991; England and Bustin, 1998; Hurst, 1991; Bell, 1967) and some of these proprietary data have been viewed by a small number of people (England and Calon, 1991; England and Bustin, 1998; Hurst, 1991; Bell, 1967).

The seismic hazard around the Strait of Georgia is not well known. In the Puget Sound region south of the Strait of Georgia, several major faults (Seattle Fault, Tacoma Fault, South Whidbey Island Fault Zone) are recognized as active, with the seismicity accommodating northeast-southwest oriented shortening associated with subduction of the Juan de Fuca oceanic plate and northward migration of the Coast Range block (Wells et al., 2003, 1998, 1988). Previously the Devil's Mountain fault, possibly connected to the Leach River Fault on Vancouver Island, was thought to be the northern extent of this active deformation. However, recent paleoseismic work has shown Holocene fault activity further north on the Vedder fault (Barnett, 2006) and the newly discovered Sandy Point and Birch Bay faults (Kelsey et al., 2012).

Geodetic observations by McCaffrey et al. (2012) and Mazzotti et al. (2002) suggest deformation still further north, well past Vancouver, British Columbia, but deformation directions conflict. Several $\geq M_L$ 5.0 earthquakes have occurred in the Puget Lowland area of the Cascadia forearc over the last 150 years (e.g., Dewberry and Crosson, 1996) but the strait is seismically relatively quiet. Shallow (<30km) seismic activity is greatest at the south end of the Strait of Georgia, in the area where the strait borders the San Juan Islands. Vancouver Island also experiences a diffuse scatter of seismic activity.

Seismic hazards around the Strait of Georgia are of concern because of potentially amplified ground motions. On 24 June 1997 a M_L 4.6 earthquake occurred ~37km WNW of Vancouver British Columbia; no significant damage was recorded for the event. Cassidy and Rogers (1999) combined strong motion recordings from the greater Vancouver area with those from the 1996 M_L 5.1 earthquake near Duval, Washington to provide the first strong motion site characterizations for the greater Vancouver area. Cassidy and Rogers (1999) performed spectral analyses and had four major findings: 1) ground motions on the Fraser river delta are amplified 2-6 times relative to those of firm soil (firm soil is the reference used by the National Building Code of Canada [NBCC]; NBCC only provides for a base shear amplification of two for thick soils [>15 meters]); 2) the largest amplifications are observed near delta edges where Quaternary sediments thin and soil resonance frequencies approach that of common building heights; 3) source and path effects play an important role; and 4) frequencies greater than 8 Hz are slightly attenuated while 1.5 to 4 Hz are amplified, suggesting small one or two story structures on delta material would experience slightly reduced shaking at their resonant frequency while three to seven story buildings on delta material would experience amplified shaking. Path dependence currently is thought to be highly variable due to extensional structures (England and Calon, 1991; England and Bustin, 1998; Bell, 1967) in a compressional setting (McCaffrey, 2012; Mazzotti, 2002).

Recent GPS studies along the Cascadia forearc have shown long-term north-south shortening extending into the Strait of Georgia, well north of recognized geologic structures known to be accommodating this north-south strain (McCaffery et al., 2000, 2002, 2012; Mazzotti et al., 2002, 2003). Detailed studies show north-south shortening can not be replicated with linear strain models, suggesting complex deformation (Mazzotti et al., 2003). Kelsey et al. (2012) documents the first Holocene surface displacements within this region, but the structures

responsible for these displacements remain poorly constrained. To better constrain geologic structures and seismic hazards spanning the border, the U.S. Geological Survey and the Geological Survey of Canada jointly conducted two marine geophysical surveys under the Seismic Hazards Investigation of Puget Sound (SHIPS) project. A cruise in 1998 collected deep marine seismic profiles using large airgun sources (Brocher et al., 1999; Fisher et al., 2005), and a second cruise in 2002 collected high-resolution seismic reflection profiles in the Strait of Georgia (Brocher et al., 2003). Reflection seismic profiles from the SHIPS cruises along with previously unpublished academic and industry reflection lines are combined here to gain insight about the structures and tectonics of the region. This study reviews new and existing marine reflection seismic profiles to: 1) search for active structures capable of accommodating observed GPS strain; and 2) examine structures proximal to recorded Holocene tectonics.

Chapter 2. TECTONIC SETTING & STRATIGRAPHY

2.1 TECTONIC SETTING

Presently the northern Cascadia region appears to be dominated by NE-SW contraction due to inter-seismic locking of the subducting Juan de Fuca plate beneath North America (McCaffrey et al., 2012) and northward motion of the Oregon and Washington coast range block (Wells et al., 1988). This contraction is partitioned on E-W striking thrust faults and NW-SE oblique or strike-slip faults in the Puget Sound region (Johnson et al., 2004, 2001, 1999, 1996; Pratt 1997; Sherrod et al., 2008; Johnson et al., 1996). Subduction related deformation approximately equal to that within the Puget Sound region appears to extend into southwest British Columbia based on GPS strain data (Mazzotti, 2011, 2002; McCaffrey 2012, 2005, 2000), but the structures accommodating this strain near the U.S.-Canadian border remain largely unidentified. From a first order perspective, the region is geometrically complex with a sweeping 35º change in the trend of the convergent margin in map view, requiring motion both parallel and normal to the subduction margin over at least half of the combined Strait of Georgia and Puget Sound region for the last 65 million years.

Tectonic theories for the Georgia basin have been substantially evolving over the past forty years. Forearc models have been the most popular (England and Calon, 1991; England and Bustin, 1998; Dickinson, 1983; Muller and Jeletzky, 1970; Bell, 1967) with northwest striking normal faults along the east and west edges of the basin to provide continuous accommodation space. Patch (1984) proposed a strike-slip basin model, but foreland basin models subsequently have gained popularity (Mustard, 1994; Monger and Journeay, 1992; Brandon et al., 1988) with the recognition of thrust sheets controlling the basin's structure, specifically the Cowichan Fold and Thrust Belt that forms east Vancouver Island and the Gulf Islands.

In summary, the margin is currently defined by the 35º change in the plate boundary caused by westward migration of the coast range block (Wells et al., 1998), has a long history of oblique convergence that has caused a variety of faults of largely unknown motion, displays ongoing deformation, locally displays tensional structural features, and hosts a NE-SW shortened fold and thrust belt.

2.2 STRATIGRAPHY

A thick sedimentary sequence composed of Cretaceous to Holocene strata underlies the Strait of Georgia. These strata consist of four major units: 1) Quaternary sediments; 2) non-marine Eocene sedimentary strata; 3) marine Cretaceous sedimentary strata; and 4) basement rocks.

2.2.1 *Quaternary Sediments*

Quaternary sediments are subdivided into modern Fraser River sediments, glacial deposits, and pre-glacial deposits. Fraser sediments are located primarily near the river mouth where they form the Fraser River delta. Glacial and pre-glacial strata are present throughout the Strait of Georgia basin and have large variations in thickness. Glacial strata represent several events throughout the Fraser glaciation. Reflection characteristics for Quaternary sediments have been described by Hamilton (1991), Hart et al. (1995), Mosher et al. (1995) and Mosher and Hamilton (1998). A prominent unconformity defines the base of the Quaternary sediments.

In my interpretation I define the different Quaternary units based on their seismic character and the presence of unconformities (figures 4e & 4f). Methane hydrates locally cause bright reflections from within the Holocene strata. Multiple units within the Holocene can be identified on seismic sections; however, multiple glacial events have cut the deposits making it difficult to link one isolated unit to another with certainty. No faulting or other deformation has been observed where dividing the Quaternary strata into finer increments would be helpful for interpretation, and the units are therefore left undivided for this study. The uppermost major sediment unit, which is easily identifiable and has good lateral continuity, is the Holocene sediment supplied by the Fraser River (Mosher et al., 2002; Hill, 2008).

2.2.2 *Eocene Chuckanut/Huntingdon Formation*

Below the unconformity at the base of the Quaternary, Eocene sedimentary strata consist of a non-marine unit deposited unconformably on the Cretaceous Nanaimo Group (figure 2; Mustard, 1994, 1991; Mustard and Rouse 1994). The Eocene unit is named Huntingdon in Canada and Chuckanut in the U.S. and has previously been mapped on the North America mainland, along the length of the Canadian Gulf Islands, and south into the San Juan Islands

(Johnson, 1991, 1984). The unit consists of arkosic sandstone with increasing lithic content moving up section, and was deposited within a series of meandering river environments throughout the Eocene.

The base of the Eocene strata is an unconformity with the Cretaceous Nanaimo, but has no distinct reflector signature on seismic profiles. Boreholes provide stratigraphic control, and continuous reflectors are used to map the strata. Continuous bathymetric bedrock ridges combined with terrestrial geologic mapping characterize the unit's base as an angular unconformity also with the Cretaceous Nanaimo.

Compressional deformation is recognized from folds within the Eocene strata (Johnson, 1984; Hurst, 1991), but the amount of shortening has not been estimated reliably (Johnston and Acton, 2003).

2.2.3 *Cretaceous Nanaimo Group*

The Cretaceous Nanaimo Group is a package of marine sedimentary bedrock up to 4 km thick (Mustard, 1994; England and Calon, 1991). Eleven units are recognized, composed of sandstone-conglomerate units alternating with mudstone and fine grained sandstone beds. Coal bearing facies serve as indicators of shallow, low energy marine deposition. Initially local basement-supplied sediment was deposited as a submarine depositional fan, driven by gravity flows. Subsequently the Coast Belt to the east and the northwest Cascades supplied the bulk of the sediments, with the eastern Cordillera also becoming a significant source towards the end of deposition. A series of northwest striking thrust faults in the Gulf Islands, known as the Cowichan Fold and Thrust Belt (England and Calon, 1991; England, 1989), displace the Nanaimo group and locally thicken the Nanaimo on Vancouver Island and the Gulf Islands. Restored cross-sections suggest up to 30% shortening (England and Calon, 1991). The Cowichan Fold and Thrust Belt is cut by a series of younger, orthogonal northeast striking "secondary faults" England (1989; England and Callon, 1991) with unclear senses of motion.

On our seismic profiles, the Nanaimo group appears as continuous reflectors indistinguishable from Eocene strata.

2.2.4 *Basement rocks*

Basement rocks bound the Georgia basin, with the Wrangellia terrane to the west, the North Cascades Terrane to the east, and the Crescent Terrane to the south. On Vancouver Island,

Wrangellia rocks are composed of arc-related volcanic rocks and sedimentary strata showing little metamorphism, with local igneous intrusions (Monger and Jouneay, 1994). The North Cascades Terrane consists of several units exposed on the mainland and in the San Juan Islands. Eocene basalt of the Crescent Terrane crops out on the southern and western edges of Vancouver Island (Monger and Jouneay, 1994).

Chapter 3. DATA

Unpublished and previously published seismic reflection data, cross sections from seismic tomography models, map layers and earthquake hypocenters were digitally integrated for this study using a 3-dimensional exploration geophysics interpretation package. Data from the 1998 and 2002 SHIPS projects were partially processed and then interpreted here; the 1998 data have been previously examined in a cursory fashion (Brocher et al., 1999; Mosher et al., 2000). Cruise track geometry was processed with MatLab, and Seismic Unix was used for seismic data processing. figure 1 shows the tracklines of the various seismic surveys used in this study.

3.1 SEISMIC REFLECTION PROFILES

3.1.1 *2002 SHIPS*

The United States Geological Survey (USGS) and Geological Survey of Canada (GSC) conducted a joint subsurface study aboard the Canadian Coast Guard vessel *John P. Tully* through the San Juan Islands, north through the Strait of Georgia, and crossing the epicenter of the 1997 magnitude 4.6 earthquake. The early portion of the cruise was used to debug a 24-channel streamer, during which time single-channel airgun data were collected ("Teledyne" data) as well as high-resolution profiles using a 3.5 kHz system or a towed "Huntec" system. The GSC's MUSE recording system multiplexed the data into a single file. Either Huntec or 3.5k kHz were alternately collected because the systems interfered with one another; generally Huntec was collected during the day and 3.5 kHz at night due to personnel schedules. The MUSE recording system is a unique system developed in-house on a SUN Ultra 10 workstation and includes a machine dependent code. Seismic profiles 8 and 10 consist of scanned paper printouts of the profiles but no digital data, as the recording system was temporarily not functioning while these profiles were collected. Appendix A and B augment Riedel's (2002) cruise report listing available digital single channel airgun data. Navigation for SHIPS 2002 data and meta data used the digitizing of paper printouts.

The GPS units periodically recorded erroneous locations, which are immediately apparent when plotted on a map. Despite both the GPS receiver and the airgun being tied to the same trigger system, the times for GPS and airgun shots do not perfectly coincide. To determine the airgun shot locations, shot times were extrapolated from the GPS positions. GPS locations

recorded the ship's location, not the airgun or streamer, so shot locations were computed to be 30 m behind the GPS position. Triggers for the 3.5 kHz and Huntec systems occurred more frequently than GPS locations were recorded, and the locations were therefore extrapolated between the GPS points.

To rectify the navigation with the data, functions for piecewise splines were fit to the GPS data to allow any location along the cruise track to be approximated; time was the independent variable in these spline functions. Erroneous GPS locations mentioned earlier were infrequent enough to not have a noticeable effect on the spline fitting when examining GPS locations on either side of the erroneous location. All instrument locations were assigned based on assuming a location of the GPS receiver on the ship and assuming a tow distance behind the ship, resulting in the GPS being about 30 m in front of the source and receiver. For a given shot time an interpolated location for the GPS receiver was calculated from the spline fitting, and time was iteratively decreased (locations behind the ship occurred earlier relative to where the ship is) until a location within approximately a meter of the tow distance was found. Locations assigned to the data headers via this method were then extracted and are the locations present in the Google Earth KMZ files; the Excel spreadsheet holds the original GPS data.

3.1.1.1 Single Channel airgun profiles

A single 80 cubic inch airgun was the source for the SHIPS 2002 recordings made with the single channel receiver. Shots were approximately every 5 seconds with a record length of 2 sec (Riedel, 2006). Processing consisted of bandpass filtering (30 to 360Hz), deconvolution with a minimum gap length of 6 milliseconds, Stolt (*f*-k) migration, and time-to-depth conversion. No stacking velocities were available from the single-channel data, so velocities for migration and depth conversion were estimated from previous studies (Hurst, 1991; Tiffin, 1969) and generic values for unconsolidated sediment, glacially overridden material, and sedimentary rocks. Velocities of ~1600m/s for unconsolidated, ~1800 m/s for glacially overridden, and 2,000 – 4,500 m/s (increasing with depth) for sedimentary rock were used for processing. The water bottom, unconsolidated sediments, and glacial sediments were well imaged.

3.1.1.2 Huntec

The Huntec system is a deep-towed acquisition system whose towfish depth was varied depending upon the water depth. The data have a 525 millisecond trace length and sample rate of

40 microseconds (Riedel, 2002). Noise frequencies overlapped or were very near the signal frequency, making bandpass filtering largely ineffective. Deconvolution with the full frequency spectrum greatly reduced wavelet sidelobes, creating sharp reflections from the water bottom. Penetration of unconsolidated sediments was achieved; bedrock penetration was limited.

3.1.1.3 3.5kHz

3.5kHz has a transmit interval of 0.5 seconds for shallow water and 0.75 seconds for deep water (Riedel, 2002). Data have a very similar appearance to the Huntec data and were likewise processed with deconvolution but no bandpass filtering. No limited subbottom penetration was achieved.

3.2 LEGACY DATA

3.2.1 *1971 Western Geophysical*

In 1971 Western Geophysical Incorporated (WGI) collected multichannel airgun profiles covering the area north of the San Juan Islands, south into Puget Sound, and west through the Strait of Georgia[1]. A large explosive-gas seismic source similar to an airgun was used. The data were provided as stacked sections after processing by WGI. The data presented here were bandpass filtered (5 to 40 Hz), and Stolt migration and depth conversion were carried out. Velocities were estimated using published borehole velocities, results of refraction tomography studies in the area (Dash et al., 2007; Zelt et al., 2001), and by trial migrations using a range of velocities defined by the uncertainties reported with borehole and tomography velocities. Shallow sediments are not well resolved because of the large seismic source, but deeper reflectors from sedimentary strata are quite strong to depths of approximately 6 km.

Locations were determined using LOng RAnge Navigation (LORAN) radio technology. LORAN uses low frequency radio signals from land stations to triangulate a location; the large relief and complex geometry of the San Juan Islands distort radio ray paths and introduce errors to the locations as these low frequency waves bend around the islands. Plotting the recorded locations suggests a very jittery track line whereas the ship actually took a generally straight

---

Data are available at: http://walrus.wr.usgs.gov/infobank/w/w270ps/html/w-2-70-ps.meta.html

track. Linear r^2 regressions were performed on raw track line locations to provide a more realistic geometry for 3D interpretation. figure 1 shows these interpolated track line geometries.

3.2.2 *Sparker seismic data*

Seismic reflection data using a 300-Joule sparker electrical source were collected off the *R/V Centennial* in 2004. Data were processed using a 180-600Hz bandpass filter, deconvolution (gap=0.002s), and time-to-depth conversion. Again the single-channel data provided no velocity control, so the velocities were assumed to be 1480 m/sec for the water and 1600 m/sec for the shallow sediments. Penetration was about 100 m into the shallow sedimentary strata.

3.2.3 *1998 SHIPS*

The 1998 cruise was conducted aboard University of Washington's *Thomas G. Thompson* research vessel throughout the Strait of Georgia, Puget Sound, and Strait of Juan de Fuca. Both multichannel reflection data and refraction data using land-based receivers were collected (Brocher et al., 1999). Thirteen airguns combined for a 79.3 liter source were recorded on a 2.4-km- long, 96-channel streamer (Fisher et al., 1999). Hydrophone group spacing was 25 meters with the nearest channel towed 200 meters behind the stern. Only the reflection data across the Strait of Georgia, lines SG1N and SG1S were used in this study, although the tomography model in the region also included data from this cruise. These lines have considerably better depth penetration than the 2002 single channel data, and the northern line passes within 4km of the epicenter of the 1997 earthquake, offering the best chance to image the fault responsible for that event. Reflection data were already stacked, and velocities were estimated from tomography models (Dash et al., 2007; Zelt et al., 2001). Data were bandpass filtered (3-36 Hz), deconvolved (gap=0.045s), Stolt migrated, and depth converted.

3.3 TOMOGRAPHY DATA

To aid the interpretation, TIFF images of the published cross-sections through the tomography models and geologic cross sections were converted to SEGY data, assigned locations, and imported into the 3-D interpretation software as seismic profiles with the amplitude being the image of the published cross section. Cross-sections included England and Callon's (1991) Nanaimo balanced interpreted cross sections, Dash et al.'s (2007) tomography sections, Zelt et al.'s (2001) tomography sections, Johnson's interpreted Chuckanut sections,

Tiffin's interpreted line tracings of past sparker lines, and the analog industry seismic lines published in England and Bustin (1998) and Hurst (1991).

Chapter 4. INTERPRETATION

Once the data were imported into the 3D interpretation software, they were analyzed by picking key horizons and unconformities, interpreting faults, and creating isopach maps. Borehole data, surface mapping, and high-resolution bathymetry were used to assign lithologies to reflector packages.

Due to the complex geometry and sparse stratigraphic control only four units are considered here: 1) Quaternary sediment; 2) sedimentary Eocene Chuckanut (US)/Huntingdon (Canada) bedrock; 3) sedimentary Cretaceous Nanaimo bedrock; and 4) basement. Interfaces between Quaternary sediment and sedimentary bedrock were identified by angular unconformities with high reflection amplitudes, with the high reflection amplitudes indicating an interface with a large velocity and/or density change. Contacts between Eocene and Cretaceous material are solely based off borehole stratigraphy or by connecting surface mapping with seismic profiles, with continuous bedrock ridges being evident on high resolution bathymetry. No reflectors from within basement material were imaged on the seismic profiles.

4.1 Major Geologic Structures beneath the Strait of Georgia

In this paper I focus on the geologic structures that form the major elements within the Georgia Basin, and the structures that have Holocene activity documented either from seismicity or from paleoseismic studies. The former include the Nanaimo Basin and Outer Isles fault; the latter include the Sandy Point structures and the fault responsible for the 1997 earthquake. Here I describe these structures as imaged by the seismic data.

4.2 Nanaimo Basin

The deepest portion of the Georgia Basin is a thick subbasin, the Nanaimo Basin, whose edges are defined by distinct folds in the sedimentary strata. The edges of the Nanaimo basin are defined by the transition from shallow Eocene strata within the basin to older Nanaimo group outside of the basin. The eastern most of Canada's Gulf Islands, Tumbo Island, is the only outcrop of Eocene bedrock observed in the Gulf Islands (figures 3 & 7); everything to the west is Cretaceous Nanaimo strata, leaving a 600 meter window between Tumbo and Satuma Islands for the contact's location. Tumbo Island is a small knob that forms part of a long ridge that can be traced continuously north along Vancouver Island's coast; this ridge intersects the 1998 SHIPS

track, providing stratigraphic control for the seismic profiles. Nanaimo Basin is defined by continuous reflectors stairstepping down from both the north and south, with the deepest portion occurring near the international border (figure 2). Reflector curvature tightens with stratigraphic depth, eventually becoming kinkbands in Cretaceous bedrock. No sharp truncations of reflectors are observed to directly indicate blind thrust systems controlling the basin, but such faults can be inferred below the edges of the basin based on the downward-sharpening fold axes.

The southern system of folds is inferred to be the offshore extension of the San Juan Thrust System, extending it 40 km further north than currently recognized. The northern Vancouver Fold and Thrust system has not previously been fully described (figure 2). Pairing of mapped bedding surfaces of the 1998 SHIPS profile with bathymetric bedrock ridges provides a northeast-southwest strike for the thrust system (figure 3). Extending to the west the surface traces of faults and folds interpreted here shows them paralleling faults labeled as "secondary" by England and Callon's mapping (1991) of the Nanaimo group (figure 3). England and Callon (1991) show these secondary faults cutting the Cowichan Fold and Thrust Belt.

The southern tip of the Vancouver Fold and Thrust Belt (VFTB) shows a narrow band of well-defined growth strata (figure 2, blue lines). These growth strata are interpreted to result from a blind, listric thrust fault that steepens as it nears the surface. Lower portions of imaged Cretaceous strata appear to have reflectors meeting at abrupt angles with no curvature, which indicates the reflectors are cut by faults. Approximately the upper kilometer of Cretaceous strata shows folding of continuous reflectors, with reflector curvature increasing with depth; growth strata continue into overlying Eocene strata. Quaternary deposits show a slight (<1º) dip, also consistent with growth strata. Back-limb geometry is not as well defined as forelimb structures but are still present. Possible on-lapping strata are highlighted in cyan (figure 2).

Non-parallel reflectors are present at the northern extent of the San Juan thrust system and are deformed by younger faults up-dip. The length of non-parallel reflectors suggests deformation on a scale larger than the seismic section.

Post-Eocene basin shortening is estimated using the Cretaceous-Eocene unconformity. Over a linear distance of 46 km the unconformity measures 46.136 km (figure 2). Lack of on-lapping strata and constant thickness of basal Eocene reflectors indicate a flat depositional surface, allowing for an estimate of a shortening rate of 146 meters over 56 million years, or 0.0026 mm/yr. There is greater deformation present in Cretaceous strata further north; however,

displaced and highly deformed reflectors do not allow specific stratigraphic units to be traced across faults to determine displacement rates. Cowichan Fold and Thrust Belt deformation likely exists between what is mapped on Vancouver Island and the seismic profile, making the extrapolation of on-shore mapped units to the seismic section tenuous. North-south deformation is further examined in subsequent sections.

4.3 Outer Island Fault

The origin of the present day Strait of Georgia basin has been debated since the beginning of subsurface investigations. Originally thought to be a graben resulting from a decrease in the convergence rate of the Farallon Plate (England and Bustin, 1998; Bell, 1967), the notion of normal faults of large enough scale to account for observed basin depth has been contested for two main reasons. First, no other normal faults are recognized parallel to the convergent margin - faults are thrust or oblique reverse. Second, the Nanaimo and Chuckanut/Huntingdon were deposited in a proto Strait of Georgia and appear to subsequently be uplifted and deformed by compression (England and Calon, 1991; England and Bustin, 1998; Johnson 1984), thus requiring down-drop for accommodation space, uplift to present terrestrial positions, then down-dropping of present day Strait of Georgia to present bathymetric expression, with erosion and/or non-deposition of Oligocene and Miocene strata along the way.

The southwest margin of the Georgia Basin, formed by the Outer Island fault, was originally interpreted as a normal fault. This notion was inferred from steeply northeast dipping beds on the western edge of the Gulf Islands, interpreted to be the Outer Island Fault and shown on Line 8 in England and Bustin (1998). The extensional nature of the Outer Island Fault was subsequently questioned because a high velocity region appeared to be uplifted west of the OIF trace in Dash et al.'s (2007) velocity model of the Georgia Basin (figure 6). With the boundary of the high velocity zone appearing near-vertical at the south end of the Gulf Islands and becoming southwest dipping at the north end of the Gulf Islands, Dash et al. (2007) reinterpreted motion on the Outer Island Fault to be blind reverse. Bedrock strata observed in Tiffin's (1969) profiles also support the blind thrust hypothesis by showing a series of folds that have greater amplitude and wavelength progressing northward along Dash et al.'s (2007) OIF proposed trace (figures 6 & 7). Furthermore, Gabriola Island (Doe, 2012) and Sucia Island (Mustard, 1994)

show syncline-anticline complexes, suggesting that deformation from the Outer Island Fault extends further north and south than the extent proposed by Dash et al. (2007).

I interpret the Outer Island fault as a blind, southwest dipping thrust fault, as proposed by Dash et al. (2007), that causes a kink band in the Cretaceous and Early Eocene strata long the eastern edge of the Gulf Islands (figure 7). The northeast-dipping strata within the kink band accounts for the relatively steep bathymetric slope moving away from shore, and for the relatively steeply dipping bedrock strata reported by England and Bustin (1998). The kink band is consistent with forelimb strata within a fault propagation fold (Suppe and Medwedeff, 1990; Shaw et al. 2005). There are no growth strata indicating post-Early Eocene deformation. Bedrock reflectors fade rapidly at the base of the kink band, leaving the larger east-west bedrock structure undefined and not permitting slip rate estimates. Overlying Holocene sediments show occasional non-horizontal reflectors between horizontal reflectors, suggesting a non-tectonic origin for non-horizontal reflectors and no obvious Holocene motion on the fault.

The southwest dip inferred for the OIF makes it antithetic to the current geometric interpretation of the Cowichan Fold and Thrust Belt on Vancouver Island (figures 3, 7, & 9). The OIF thus appears to be a backthrust to the Cowichan fault system, or vice-versa.

4.4 1997 Gabriola Earthquake

The seismic hazard of the Georgia basin was re-evaluated following a M_L 4.6 thrust earthquake on 24 June 1997. This earthquake was preceded by a M_L 3.4 foreshock on 13 June. Although these earthquakes did not cause any significant damage, their location within 37 km of the city of Vancouver (Cassidy and Rogers 1999) raised the question of whether the faults responsible for these earthquakes could host much larger earthquakes, could extend directly beneath the city, or could be part of a more extensive fault system that does extend beneath the city.

Focal mechanism solutions from P-nodal (Cassidy et al, 2000) and centroid moment tensor (CMT) (Malone et al., 1997) were computed for both the foreshock and mainshock. The P-nodal solution shows the mainshock ruptured a 47º north dipping fault striking 262º with a slip of 98º; the CMT solution differs slightly with a dip of 56ºN, strike of 278º and slip of 120º. The CMT foreshock solution is a 67º north dipping thrust, striking 259º with a slip of 109º, similar to both solutions for the mainshock. However, first motion data for the foreshock allow

significantly different fault and slip geometry from P-nodal solutions. Solutions range from a geometry similar to the mainshock solutions (strike 236, dip 43, slip 123), all the way to a north dipping right lateral strike-slip fault (strike 266, dip 72, slip 156). Cassidy's (2000) relocation of 55 aftershocks is best described by a plane dipping 47 degrees to the north, suggesting a north-northwest striking thrust fault dipping approximately 45 degrees best describes the fault and motion of the 1997 earthquake mainshock.

The 1998 SHIPS profile crosses within approximately 3.6 km of the hypocenter along a NE/SW track (figure 4a), which is oblique to the assumed fault plane. Projecting the relocated earthquakes onto the SHIPS 1998 profile places them near a group of interpreted faults, marked by reflector terminations with deformation of shallow sediments above (figure 4b & 4c) not imaged on previous versions of the profile (figure 4d). The reflector terminations and fold geometry are consistent with fault-propagation-fold geometry, agreeing with the stress states derived from the focal mechanisms. The seismic profile shows six splay faults reaching the bedrock-sediment interface and extending down 500 to 2000 meters before reflector coherence is lost. A slightly listric fault dipping approximately 45º to the northwest is interpreted to reach greater depths and form the master fault based upon northwest dipping reflector termination planes north and south of the earthquakes, and on the focal mechanism solutions. The three largest splay faults are antithetic to the listric main fault (figure 4c).

Above the bedrock deformation in the vicinity of the 1997 earthquake, the SHIPS 2002 seismic data image triangular blocks of displaced sediment (figures 4e & 4f). Blocks are approximately 800 meters wide at the sea floor and at least 100 meters tall. Vertical displacements are on the order of meters, approaching the resolution of the data. A distinct failure plane cannot be traced to bedrock; however, sediment surrounding the blocks also appears tilted, suggesting bedrock fault block motion transitions to soft sediment deformation of Quaternary deposits; when internal strain becomes too great blocks of sediment may locally fault. These triangular blocks can be traced across all of the 2002 SHIPS lines (figure 4a) and trend 10º north of west. The trend of the faults bounding these displaced sediment blocks projects onto an unnamed fault mapped on Vancouver Island, passing between the north end of Gabriola Island and the Hudson Rock Ecological Reserve. Both P-nodal and CMT moment solutions strike slightly south to the Leboeuf Bay and Drangon's Lane faults (Doe 2009, England and Bustin, 1998), cutting Gabriola Island (figure 4). All three of these faults have previously

been considered either normal or strike-slip despite dramatic changes in bedrock dip angles across each fault. Because of the splay fault geometry present in the bedrock it is possible that all three faults were active during the 1997 earthquake.

On the SHIPS 1998 line no distinct reflector packages within the 1500 meters of well imaged strata (figure 4b) can be correlated across the main fault, which allows for two possible interpretations of fault motions. The first interpretation is that post-Cretaceous vertical displacement is greater than 1500 meters. The second interpretation is that the combination of out-of-plane bed thickness variation and strike-slip motion is great enough to not allow reflectors to be correlated on the seismic section. Bed thickness variations could be the result of deposition mechanisms or earlier deformation caused by the Cowichan Fold and Thrust Belt. Shallow deformation observed on the grid of 2002 SHIPS lines, combined with bedrock deformation observed on the 1998 SHIPS line, establish a minimum fault length of 18 km, with an imaged width of 2.5 km.

Despite only slight ambiguity in the trend of the faults, focal mechanism solutions suggest 10º south of west while Holocene sediment deformation observed on the 2002 SHIPS airgun lines suggests 10º north of west, the pervasiveness of faulting throughout the region impedes definite correlation of onshore mapped faults with those observed here in section. Projecting the fault defined by the focal mechanism solutions ~20 km east places the fault under West Vancouver. Holocene sediment deformation projects to Sea Island British Columbia, just south of Vancouver and home to Vancouver International Airport.

I prefer a northeast strike interpretation for the faults because focal mechanisms and onshore bedrock faults match this orientation and attribute the slight skew of the band of sediment deformation to preexisting sediment fabric. This interpretation identifies the Lebeouf Bay and Dragon's Lane faults on Gabriola Island as active and potential sites for future neotectonic studies.

4.5 Sandy Point Structures

Kelsey et al. (2012) first identified three northwest striking faults, the Sandy Point, Birch Bay, and Drayton Harbor faults, near the US/Canadian border based on LiDAR visible fault scarps, sharp gradients in the magnetic field, changes in diatom species, and uplifted beach

terraces (figure 5a). Holocene vertical displacements of meter scale were interpreted from elevation changes of marshes, suggesting fault slip of similar amounts. figure 5 shows the senses of motion interpreted for the faults (Kelsey et al., 2012). Elevation changes are interpreted from changes in diatom species.

Western Geophysical lines W2 (figure 5b) and W3 (figure 5c) cross the projected locations of the Sandy Point and Birch Bay faults. Both lines stretch from just south of the US/Canadian border into the northern San Juan Islands and the associated San Juan thrust system (figure 5a). Hydrocarbon exploration well AHEL provides stratigraphic age control, which is then projected onto W2 and W3 by correlating similar reflector packages; deformation imaged on line W4 (figure 5d) accounts for the difference of stratigraphic depths on W2 and W3. Seismic profiles show that beneath Quaternary sediments of varying thickness (0-300 meters), a gently deformed, approximately 3-km-thick sedimentary bedrock sequence dominates the northern portion of the lines.

The Birch Bay Fault forms a sharp inflection point and reflector truncations at the northern end of line W3 (figure 5c). Reflectors correlate across the kink, indicating little to no net vertical displacement on the fault. Deformation around the kink increases with depth, consistent with growth faulting, to approximately 4km where reflector coherency near the end of the line is lost due to migration edge effects.

The southern extent of the horizontally-stratified sedimentary rocks is defined by an abrupt termination that is either a fault, a sharp fold, or both. Strata to the south of the fault appear to be dipping 10^{o} northward. The strike of the abrupt termination of strata on the seismic profile coincides with the projected location of the Sandy Point fault as interpreted from the trends of magnetic anomalies that coincide with the on-land location of the fault (Kelsey et al., 2012).

Reflectors on profile W3 abruptly flatten at 3.5 to 4km depth relative to overlying reflectors. Additionally, reflectors can be traced beneath the Sandy Point Fault suggesting the upper strata are a block sitting on a detachment. Consistent reflector geometry within the bedrock allows for interpretation of the unconformity at the top of the Nanaimo Group. Based off this projection approximately 1.5 km of Eocene aged Chuckanut overlies approximately 1.5 km of Cretaceous Nanaimo, if the change in reflector geometry at ~3.75 km is interpreted as a

detachment. Generally parallel Eocene and Cretaceous strata suggest a paraconformity with approximately 10 million years worth of absent stratigraphy.

This 1500 meter thickness of Chuckanut strata is consistent borehole data (Hurst, 1991) but conflicts with the 6,000 meter thickness derived from surficial mapping. This discrepancy combined with generally flat lying strata in a region of thrust sheets (Mustard, 1994; Mongery and Journeay, 1992; Brandon et al., 1988) could be reconciled by interpreting the area as a foreland dipping duplex (Boyer and Elliott, 1982).

Reflectors crossing beneath the Sandy Point fault are interpreted to be real rather than sideswipe based on two observations. First, shorelines are closer at the northern end of line W3 and no sideswipe artifacts are present. Second, these reflectors respond in the same way as the upper Cretaceous and Eocene reflectors when the velocity functions used in processing are changed. If processing velocities are set to 1500m/s, the propagation speed of water, sideswipe artifacts from passing the San Juan Islands appear within the upper section of the southern portion of line W3; reflectors passing below the Sandy Point Fault and upper Cretaceous and Eocene reflectors disappear due to the improper velocity profile. When processing velocities are within the standard range of 2000-4000 m/s for sedimentary bedrock the San Juan Island sideswipe is not pronounced and reflectors passing beneath the Sandy Point Fault become strong along with Cretaceous and Eocene reflectors.

South of the Sandy Point Fault bedrock reflector coherence is poor with the exception of bedrock knobs poking to the surface. Detailed mapping of the San Juan Islands is carried offshore via a 5-meter bathymetric mosaic to identify reflectors as Eocene and Cretaceous. In map view, a high magnetic anomaly (Kelsey et al., 2012) corresponds with the area of poor reflector coherence in W3. There is no similar magnetic high located where reflector coherency is lost on W2, suggesting that the cause of coherency loss must be of larger scale, possibly beds dipping at steep angles or a western extension of the “tectonic zone” mapped on Lummi Island (Schuster, 2005).

Lines San Juan 1 (figure 5e) and San Juan 2 (figure 5g) from the *Centennial* sparker surveys show the most recent 10 meters of sediment above Sandy Point structures being unbroken and of constant thickness. The upper 10 meters of sediment sits on an angular unconformity at the top of older Quaternary sediment. On San Juan 2 the unconformity surface displays a 15 meter down to the south stair-step surface, and 25 meters farther down is a 5 meter

down to the north stair-step surface (figure 5h). No stair-step surfaces are present on San Juan 1 (figure 5f). Bedrock knobs pierce Quaternary sediment near the center of each line. Sediments above the knob flanks are of constant thickness and have constant slopes suggesting faulting however theses knobs are 3km south of the abrupt termination of bedrock reflectors. If sediments have been tiled by uplifted bedrock knobs, the sense of motion would agree with geometry established on lines W2 and W3 for the Sandy Point, conflicting with Kelsey et al.'s (2012) reported motions.

Extending Kelsey et al.'s (2012) Sandy Point Fault trace to the strata terminations on lines W2 and W3 indicates a fault length greater than 30km.

Line W4 (figure 5d) runs roughly orthogonal to lines W2 and W3 (figure 5a). A single fault-propagation fold deforms the northern half of the section. Forelimb and back limb structures are well defined with deformation increasing with depth indicating syndepositional compression. Another step down to the south appears just south of the crossing of line W3. Reflector curvature increases with depth and strata are onlapping. The extent of onlapping strata and variation of bed thickness make this feature is unusual compared to other tectonic features imaged on lines W2 and W3 where onlapping strata is limited and beds are of constant thickness. A northwest dipping thrust fault interpretation loosely fits the sense of deformation; however, reflector geometry does not match the forelimb and backlimb geometry observed on the northern section of the line or the SHIPS 1998 line. Thus the kinematics responsible for this step remain unresolved.

Motions interpreted for the most recent events (Kelsey et al., 2012) do not agree well with the observed subsurface fault geometries on lines W2 and W3, and the faults do not show consistent deformation progression in shallow sediments (figures 5e & 5g). These discrepencies could be due to several factors. Both the Sandy Point and Birch Bay faults are blind faults on shore (Kelsey et al, 2012) so the lack of a bathymetric scarp is not unreasonable. However, folding of Quaternary sediment driven by a blind fault would still be expected. Both the Sandy Point fault and Birch Bay fault have small anticlines with tight folds beside them, the most recent events could have been related to tightening of these folds and the faults may have been locked. Lack of obvious progressively folded sediment could be due to the combined effect of the distributed folding by blind bedrock faults and the strong tidal currents responsible for large-scale sediment bedforms (Mosher et al., 2002) which might re-grade any fault-induced

bathymetric slope change before sufficient deposition can occur to preserve folded sediment. Currents appear to dominate bedforms just north of Sandy Point where the Foreslope Hills, dunes 20-30 meters high, kilometers long, wavelengths of ~700 meters, are maintained by strong currents with a large density gradient despite continuous gravity flows off the Fraser River delta periodically cutting the dunes (Mosher et al., 2002). Quaternary sediments appear to be influenced by but not a direct continuation of bedrock deformation based on SHIPS 2002 and 1998 profiles for the 1997 Gabriola earthquake, therefore short-term disconnects between surface expressions and deeper tectonic motions are plausible.

Chapter 5. REVISED BASIN MODEL

Mustard (1994) proposed the alternative forearc rather than foreland basin model because of sedimentation resulting from the thrusting of neighboring terranes, with proximity to a volcanic arc being largely irrelevant (figure 8). In the forearc model basin subsidence and geometry is controlled by interactions between the continental crust and the subducting plate. In the foreland model basin geometry results from thrusting of strata within the forearc, a basin forms where strata is least uplifted.

The foreland model is supported by observations here where the basin's large accommodation space results from rising basin sides rather than down dropping of the basin itself (England and Bustin, 1998; Bell, 1967). Folding by the Outer Island Fault and a duplexed block of Cretaceous and Eocene strata are interpreted to form the west and east edges respectively of present day Georgia Basin. Recognizing the duplexed strata slightly modifies the model to a foreland-dipping duplex (Boyer and Elliott, 1982). figure 9 provides a crude schematic model.

Long-lived northeast shortening across the Georgia basin region is evident from the series of accreted terranes and the presence of major mapped faults paralleling the subduction zone. Growth strata are likely present in the western portions of the Nanaimo basin but are likely difficult to observe in outcrop due to the degree of deformation caused by the younger Cowichan Fold and Thrust Belt.

Northwest shortening is observed in growth strata imaged on seismic line SG1 from the 1998 SHIPS cruise (figure 2) indicating it also is relatively long-lived, originating in the mid-Cretaceous at latest, and being orders of magnitude less than shortening normal to the convergent margin. A pointed driving force normal to the convergent margin is required to cause the counterclockwise rotation of the southern Outer Island Fault, and associated structures such as the Border Fault. The combination of minor NW, margin parallel shortening and localized, substantial NE deformation support Brandon et al.'s (1988) model "a" over their model "b". Model "a" proposed San Juan terrane arrival and accretion generally normal to the margin while model "b" suggested a more oblique arrival angle with significant left lateral strike-slip along the continent.

Interpreted faults and fold hinges on the 1998 SHIPS profile align with England and Calon's (1991) northeast striking "secondary faults", suggesting at least some of the existing

faults should be interpreted as oblique faults extending from offshore to the northeast, at least to the center of the Strait of Georgia (figures 3 and 7).

Interpreting the Sandy Point Fault as the termination of a duplexed block resulting from a northwest-directed impalement of the San Juan Islands is preferred because it fits all of the data. The localized shortening would account for the lateral overlap of Sandy Point and Outer Island Faults, allows for conflicting strata geometry on the SHIPS 1998 and Western Geophysical lines to be disconnected, and agrees with trends of the Coast Belt Thrust System (Rusmore et at., 2000) further north along the convergent margin. Duplex-generated horses could act as local hydrocarbon traps, thus explaining the eastern progression of hydrocarbon exploitation throughout the years (Hurst, 1991; England and Calon, 1991; Tiffin, 1969), and resolving Johnson's measured sections of 6000 meters (Johnson, 1985) with the ~2000 meters observed with combined surface mapping, boreholes (Hurst, 1991), and seismic sections.

A dome and basin model could also be appropriate for the region given the orthogonal fault systems. The dome and basin model would account for the different dip directions of strata on the SHIPS 1998 and W4 lines and magnetic data (Kelsey et al., 2012) forming an egg carton pattern (Theissen, 1986; Theissen and Means; Ramsay, 1967). However, deformation on the northwest trending thrust systems appears to be orders of magnitude greater than the deformation on the northeast trending systems, which is not consistent with a symmetric "egg carton" pattern of magnetic anomalies.

Chapter 6. IMPLICATIONS FOR EARTHQUAKE HAZARDS

Besides the safety of the large population and key facilities in the greater Vancouver area, accurately characterizing seismic hazards in the region is critical to understanding the threats to Vancouver International Airport and the 138kV submarine transmission line traversing the Strait of Georgia from Point Roberts to the Saanich Peninsula. The latter supplies Vancouver Island with electricity and ensures continued operation of the major infrastructure on the island.

Three geologic hazards associated with earthquakes have previously been identified for the greater Vancouver area: 1) ground shaking with soft soil amplification (Cassidy and Rogers 1999); 2) slope failure on the Fraser River delta and associated lateral spreading (Christian et al., 1997; Luternauer et al., 1994; Hart, 1993; Hamilton, 1987); and 3) tsunamis resulting from seafloor uplift or massive slope failure (Luternauer et al., 1994; Hart, 1993; Hamiltion 1987; Rabinovich et al., 2003).

Understanding the risk to common building heights of 3-7 stories and path sensitivity (Cassidy and Rogers 1999) rely on characterizing active faults, fault geometry within bedrock, and developing a tectonic model consistent with kinematic indicators observed on subsurface profiles and bathymetry. Shaking related hazards are discussed by Cassidy and Rogers (1999) and not discussed here.

Tsunami hazard has long been associated with mass wasting events off the Fraser River delta (Rabinovich et al., 2003; McKenna, 1992; McKenna and Luternauer, 1987) despite no correlation of abnormal tide gauge readings with mass events (Hamilton, 1987). A region of bathymetric dunes, the Foreslope Hills, just offshore of the Fraser River delta has recently been reinterpreted as large migrating sediment waves rather than slope failure deposits (Mosher et al, 2002). No tsunami deposits have been recognized within the Strait of Georgia, but there also has been no known study specifically searching for tsunami deposits or related studies where investigators would be likely to make the difficult differentiation of tsunami deposits from deposits similar in appearance.

For example, tsunami deposits from the 2012 M_L 7.7 Haide Gwaii earthquake were difficult to identify because the event occurred in November when winter storms off the Pacific Ocean highly reworked the beaches (Bird et al., 2013). Kelp hanging from branches in the near-

shore forests demonstrated that a tsunami occurred and provided the best indicator of tsunami heights around Vancouver Island (Bird et al., 2013).

Submarine slope failure along the Fraser River delta has been documented in the past, raising the question of whether large failures could be triggered by earthquakes. McKenna and Luternauer (1987) documented the first large, approximately 1,000,000 m^3, sediment failure off the edge of the Fraser River delta and within 100 meters of the Sand Heads Lighthouse. The lighthouse is a pile-supported structure, located within 9 km of shore, and marks the end of Steveston Jetty. Steveston Jetty sits on the north side of a maintained navigation channel across the delta to the Fraser River. The lighthouse was automated shortly after McKenna et al. (1992) proposed there is slope instability around the structure. Depth soundings performed by the Port and Waterways Engineering Survey Division of the Pacific Region of Public Works Canada to assist dredging activities on 27 June 1985 and 11 July 1985 showed dramatic changes (as much as ?? m) in bathymetry between the two surveys. Sedimentation of an unknown amount likely occurred between soundings, making the differencing of these soundings a lower estimate for the volume of failed material. Hamilton (1987) notes there are no abnormal tide gauge readings throughout the region for this period, indicating a local tsunami was not generated by the displacement of material. No seismicity was recorded by either the USGS or GSC networks between soundings, limiting any seismic event to less than M 1.0. Lacking a tsunami as an indicator of rapid failure and displacement, McKenna and Luternauer (1987) suggested the mass movement occurred as a fluid-supported sloughing of material as part of delta formation and growth.

Interpretation of the Foreslope Hills as massive slump failures that caused large scale water displacements, however, motivated the first assessments of the tsunami risk in the Strait of Georgia (Hamiltion 1987). Numerical tsunami models for hypothetical submarine failures predict wave heights of 18 meters hitting the Gulf Islands from a 750,000 m^3 failure block (Rabinovich et al., 2003). These model results, coupled with the lack of abnormal tide gauge readings for known slope failures (Hamilton, 1987), suggest submarine slope failure induced tsunamis pose a relatively small hazard. There were no large submarine failures or tide gauge abnormalities associated with the 1997 Gabriola earthquake, suggesting an event greater than M_L 4.6 would be needed to trigger a slope failure off a delta actively shedding supplied sediment with strong currents offshore, as the Fraser River delta appears to be.

The only wave of noticeable size on record within the Strait of Georgia was generated by the slumping of a sandy spit triggered by one of Canada's largest earthquakes, the M 7.3 June 23,1946 earthquake. This earthquake resulting in one death when a small boat capsized in the water wave (Rogers and Hasegawa 1978). The earthquake occurred at the north end of the Strait of Georgia (Gutenberg and Richter, 1949; Hodgson and Milne, 1951) or just to the west under Vancouver Island's east coast (Rogers and Hasegawa, 1978) at 30km depth. Rogers and Hasegawa (1978) located it well above the subduction interface (McCrory et al., 2012; Rogers and Hasegawa, 1978). The lack of a tsunami supports pure strike-slip motion (Rogers and Hasegawa 1978). Located at 30 km depth, this remains one of Canada's largest earthquakes.

The Sandy Point and Birch Bay faults define a bedrock block measuring approximately 10km by 20km beneath the Strait of Georgia (figure 5). Kelsey et al. (2012) documents 4 m of shoreline elevation change for this region. Considering the 4 meters to accumulate over several events still presents the possibility of significant tsunami hazard, with as much as 1 m of slip in a given earthquake. Given the >30km length of the Sandy Point fault documented here, and the >1 m of vertical shoreline change, empirical relations suggest that the fault is capable of M6.5 or larger earthquakes (Wells and Coppersmith, 1994).

Chapter 7. GPS STRAIN & REGIONAL HAZARD

The Devil's Mountain Fault is currently the northernmost source included on the USGS National Seismic Hazard Map (Peterson et al., 2008). Our seismic profiles combined with Kelsey et al's (2012) work shows that the Sandy Point structures extend at least 3km below the surface, have a map length of >30km, have recurrence intervals of 1,000 to 2,000 years, and have meter scale displacements. These fault parameters suggest there is substantial seismic hazard in the are north of the Devil's Mountain fault.

Mazzotti et al. (2002) estimates 5 to 6.5 mm/yr of long term north-south shortening occurring over an area stretching from southern Oregon to central Strait of Georgia. The majority of this permanent strain is geologically accounted for over the Puget Sound region (Mazzotti et al., 2002; Peterson et al., 2008), but 1-2 mm/yr, approximately 20%, remains unallocated and is taken up in either southern Oregon or in the central Georgia Basin (Mazzotti et al., 2002). Seismically active compressional features along the 1998 SHIPS seismic profile provide an explanation for at least part of this un-partitioned strain. A small strain rate of 0.0026 mm/yr is known from the deformed Cretaceous-Eocene unconformity on the 1998 SHIPS seismic line (figure 2). If the lack of reflector correlation across the 1997 Gabriola earthquake fault (figure 4) is attributed to vertical thrust motion, then 1500 meters of non-correlating strata must have been displaced since approximately the end of the Cretaceous, giving the fault a slip rate of 0.016 mm/yr. Just south of the 1997 Gabriola earthquake fault is another large fault-propagation-fold structure, with slightly more complicated geometry.

The Georgia Basin region has not been seismically instrumented long enough to accurately characterize the long-term seismicity rate (Clauge, 2002), making it difficult to establish recurrence intervals. The best estimate possible is to consider the southern Strait of Georgia, the length imaged by the SHIPS 1998 profile, as a region of shortening. The 1976 M 5.3 under Pender Island (Clauge, 2002) and the 1997 M_L 4.6 Gabriola earthquakes could be considered as events occurring on the Vancouver Fold and Thrust system and the region a tentative recurrence interval of ~M5 events until detailed neotectonic studies can be conducted on Gabriola Island.

Chapter 8. DISCUSSION

Within Georgia Basin bedrock faults have not been observed to continue into Quaternary sediments but rather displaced bedrock places stress on the bedrock-sediment interface, sediment then deforms in response to this surface loading. This surface loading can permit soft sediment deformation occurring without a planar surface connecting deformed sediment and bedrock on seismic profiles. This dynamic emphasizes the importance of strong bedrock penetration by seismic profiles when mapping faults within the basin. A sharp change in material properties, ~1700m/s sediments against ~2000m/s sedimentary bedrock, combined with possible subtle fabrics within sediments resulting from being glacially overridden is interpreted to account for this behavior.

North south deformation across the northern Cascadia forearc appears to begin abruptly in southern Washington/northern Oregon and decrease with distance north into southern British Columbia. This shortening is accommodated on fault geometries, perpendicular to the subduction margin and askew. The Tacoma fault, Seattle fault, and Vancouver Fold and Thrust Belt are the former while the South Whidbey Island fault and Devil's Mountain fault are the latter. Additional askew fault structures in the area of known Sandy Point structures could explain the disagreement between terrestrial studies and marine reflection profiles. This change in fault geometry is interpreted to result from northern migration of the Oregon block imposed on the local curving of the subduction margin. This observation suggests other curved subduction zone with an additional tectonic forcing (e.g. northern migration of the Oregon block) would also present with multiple fault geometries.

Chapter 9. FUTURE WORK

Processing of multichannel seismic reflection profiles acquired during the 2002 SHIPS cruise to better resolve bedrock faulting proximal to the 1997 earthquake as begun. Processing is expected to continue into early 2014 when interpretation will commence.

Resolving strike for the blind thrust fault imaged on line W4 could be accomplished by an additional deep seismic line, preferably askew to existing lines to better resolve apparent dip issues, extending further north within Boundary Bay. No deep seismic profile transcending the Strait of Georgia is known to have been complete; such a line would better constrain the northern extent of Sandy Point structures as well as determine off-shore deformation associated with the Cowichan Fold and Thrust Belt.

The current disparity of Eocene strata thickness from surficial mapping and reflection profiles is difficult to reconcile. Additional dating of subsurface strata could support historic subsurface dates.

Magnetic data has greatly aided tectonic studies in Puget Sound (Sherrod et al., 2008; Kelsey et al., 2012; Blakeley et al, 1995). Magnetic igneous bodies of the Coast Range Plutonic complex (Rusmore et al., 2000) complicate magnetic data north of the San Juan Islands, requiring pluton bodies be identified and removed from magnetic data when fault identification is the goal. For this reason seismic profiles would be preferred over additional magnetic surveys.

Chapter 10. CONCLUSIONS

The Strait of Georgia is underlain by a southeast trending basin that has been highly deformed locally by forearc shortening and the emplacement of the San Juan Terrane. The Chuckanut and Nanaimo are suspected to be duplexed along the west coast of the mainland based upon stratigraphic ages from industry wells and the low gravity anomaly along the eastern shore of the Strait. Continuous uplift of the east and west coasts of the strait have generated accommodation space since the mid Cretaceous, allowing for thick sedimentary sequences to accumulate beneath the present Strait of Georgia. Recognition of the basin geometry and accommodation space being controlled by fold-and-thrust belts supports Mustard's hypothesis that the Georgia Basin is a foreland basin rather than a forearc basin. Here I suggest the east edge of the Strait is formed by a foreland-dipping duplex deforming Cretaceous and Eocene Strata.

The Eocene Chuckanut/Huntingdon strata lies above a paraconformity at the top of the upper most Cretaceous Nanaimo on Lummi Island and further east in the Cascades (Brandon et al 1988) and is imaged on the Western Geophysical lines. Combiningg Nanaimo mapping (England and Calon, 1991, detailed mapping of the Chuckanut (Mustard and Rouse, 1991; Johnson, 1991), and high-resolution bathymetry indicates there is an angular unconformity between the Cretaceous and Eocene strata east of the Gulf Islands.

I propose the Leboeuf Bay fault or Dragon's Lane fault cutting across Gabriola and Vancouver Island as the most likely culprits of the 1997 earthquake To determine how close these faults might come to locations of concern for seismic hazard analyses, seismic surveys designed to penetrate roughly 1000 meters into the sedimentary Cretaceous and Eocene bedrock would be preferred over the smaller airgun profiles collected in 2002. Sediment deformation present on the 2002 SHIPS lines above the 1997 Gabriola earthquake agrees well with the focal mechanisms, but it appears this deformation resulted from internal deformation rather than a scarp resulting from the bedrock fault continuing to the sea floor.

Submarine slope failures off the Fraser River delta have yet to result in abnormal tide gauge readings despite displacements of large volumes (up to 1,000,000 m^3) (Mosher et al 2002). At least one failure occurred without recorded seismic activity, suggesting such failures are part

of the normal delta growth process. High energy currents within the Strait of Georgia may assist in preventing seismically susceptible bodies of sediment from accumulating. There is no record of tsunamis occurring within the Strait of Georgia from fault displacements during earthquakes, but shoreline elevation changes recorded by Kelsey et al (2012) and the geometry of the Sandy Point structures suggest tsunamis likely happened in the past.

The newly recognized Vancouver Fold and Thrust system is orthogonal to the Cowichan Fold and Thrust belt elevating Georgia Basin's recognized structure from a single fold and thrust belt to dome and basin. This thrust system is currently active, accommodating previously unpartitioned long-term N-S shortening.

I have identified major faults in the locations predicted for the Sandy Point and Birch Bay faults, with trends that are consistent with the trends of magnetic anomalies. The Sandy Point fault, in particular, appears to be a major boundary forming the south end of a ~3-km-thick sedimentary sequence. Reported motions on Sandy Point structures are opposite to the longer-term deformation indicated on seismic profiles, indicating complex tectonics that includes strike-slip or a reversal of motion. This suggests strain to be linear along the Gulf Islands with non-linear strain being limited to the northern San Juan Islands – southern Gulf Islands region.

These findings indicate current USGS National Seismic Hazard Maps should be modified to incorporate the Vancouver Fold and Thrust system as the northern most active structure accommodating long-term north-south shortening, approximately 100km further north and the currently northern most feature, the Devil's Mountain Fault, to more accurately represent seismic hazard within Cascadia.

References

Barnett, E. A., H. M. Kelsey, B. L. Sherrod, R. J. Blakely, J. F. Hughes, E. R. Schermer, R. A. Haugerud, C. S. Weaver, and E. Siedlecki (2006), Active faulting at the northeast margin of the greater Puget lowland: A paleoseismic and magnetic-anomaly study of the Kendall scarp, What- com County, Northwest Washington, Eos Trans. AGU, 87(52), Fall Meet. Suppl., Abstract S31A-0183.

Bell, G.L., 1967. Big potential oil basins offshore from west coast. *Oilweek*, 18(9), pp.48–57.

Bird, A., Halchuk, S. & Rosenberger, A., 2013. Shaking and Impacts from the October 2012 Magnitude 7.7 Earthquake near Haida Gwaii. *2013 Seismological Society of America Annual Meeting, Salt Lake City*.

Blakely, R.J. et al., 1995. Tectonic setting of the Portland-Vancouver area, Orgon and Washington: Constrains from low-altitude aeromagnetic data. pp.1–13.

Boyer, S.E. & Elliott, D., 1982. Thrust Systems. *The American Association of Petroleum Geologists Bulletin*, 66(9), pp.1196–1230.

Brocher, T.M., Parsons, T., Creager, K.C., Crosson, R.S., Symons, N.P., Spence, G.D., Zelt, B.C., Hammer, P.T.C., Hyndman, R.D., Mosher, D.C., Trehu, A.M., Miller, U.S., Fisher, M.A., Pratt, T.L., Alvarez, M.G., Beaudoin, B.C., Louden, K.E., and Weaver, C.S., 1999, Wide-angle seismic recordings from the 1998 seismic hazards investigation of Puget Sound (SHIPS), western Washington and British Columbia, *U. S. Geological Survey Open-File Report* 99-314, 110 pp.

Brocher, T.M., Pratt, T.L., Spence, G.D., Reidel, M., and Hyndman R.D., 2003, Wide-angle seismic recordings from the 2002 Georgia Basin geohazards initiative, northwestern Washington and British Columbia, *U. S. Geological Survey Open-File Repor*t 03-160. (http://geopubs.wr.usgs.gov/openfile/of03-160).

Cassidy, J.F. & Rogers, G.C., 1999. Seismic site response in the greater Vancouver British Columbia, area: spectral ratios from moderate earthquakes. *Canadian Geotechnical Journal*, 36, pp.195–209.

Cassidy, J.F. et al., 2010. Canada's Earthquakes. *Geoscience Canada*, 37, pp.1–17.
Cassidy, J.F., Rogers, G.C. & Waldhauser, F., 2000. Characterization of Active Faulting Beneath the Strait of Georgia, British Columbia. *Bulletin of the Seismological Society of America*, 90, pp.1188–1199.

Christian, H.A. et al., 1997. Geomorphology and potential slope instability on the Fraser River delta foreslope, Vancouver, British Columbia. *Canadian Geotechnical Journal*, 34, pp.432–446.

Clauge, J.J., 2002. The Earthquake Threat in Southwest British Columbia: A Geologic Perspective. *Natural Hazards*, 26, pp.7–34.

Clauge, J.J., Naesgaard, E. & Nelson, A.R., 1997. Age and significance of earthquake-induced liquifaction near Vancouver, British Columbia, Canada. *Canadian Geotechnical Journal*, 34, pp.53–62.

Dash, R.K. et al., 2007. Upper-crustal structure beneath the Strait of Georgia, Southwest British Columbia. *Geophysical Journal International*, 170(2), pp.800–812. Available at: http://gsa.confex.com/gsa/2009AM/finalprogram/abstract_164025.htm.

Dewberry, S.R. & Crosson, R.S., 1996. The M_D5.0 Earthquake of 29 January 1995 in the Puget Lowland of Western Washington: An Event on the Seattle Fault? *Bulletin of the Seismological Society of America*, 86(4), pp.1167–1172.

England, T.D.J., 1991. Late Cretaceous to Paleogene Structural and Stratigraphic Evolution of Georgia Basin, Southwestern British Columbia: Implications for Hydrocarbon Potential. *Washington Geology*, 19, pp.10–11.

England, T.D.J., 1989. *Late Cretaceous to Paleogene Evolution of the Georgia Basin, Southwestern British Columbia*. PhD dissertation, Memorial University of Newfoundland.

England, T.D.J. & Bustin, R.M., 1998. Architecture of the Georgia Basin southwestern British Columbia. *Bulleting of Canadian Petrolium Geology*, 46(2), pp.288–320.

England, T.D.J. & Calon, T.J., 1991. The Cowichan fold and thrust system, Vancouver Island, southwestern British Columbia. *Geological Society of America Bulletin*, 103, pp.336–362.

Fisher, M.A., Brocher, T.M., Hyndman, R.D., Trehu, A.M., Weaver, C.S., Creager, K.C., Crosson, R.S., Parsons, T., Cooper, A.K., Mosher, D., Spence, G., Zelt, B.C., Hammer, P.T., tenBrink, U., Pratt, T.L., Miller, K.C., Childs, J.R., Cochrane, G.R., Chopra, S., and Walia, R., 1999, Seismic survey probes urban earthquake hazards in Pacific Northwest, *EOS Transactions American Geophysical Union*, v. 80, no. 2, p. 13-17.

Fisher, M.A., Brocher, T.M., Hyndman, R.D., Trehu, A.M., Weaver, C.S., Creager, K.C., Crosson, R.S., Parsons, T., Cooper, A.K., Mosher, D., Spence, G., Zelt, B.C., Hammer, P.T., tenBrink, U., Pratt, T.L., Miller, K.C., Childs, J.R., Cochrane, G.R., Chopra, S., and Walia, R., 1999, Seismic survey probes urban earthquake hazards in Pacific Northwest, *EOS Transactions American Geophysical Union*, v. 80, no. 2, p. 13-17.

Gutenberg, B. and Richter, C. F. (1949). Seismicity of the Earth and Associated Phenomena, Princeton University Press, Princeton.

Hamilton, T.S., 1987. The Foreslope Hills of the Fraser Delta: Implications for Tsunamis in Georgia Strait. *Science of Tsunami Hazards*, 5, pp.15–33.

Hart, B.S., 1993. Large-scale in situ rotational failure on a low-angle delta slope: The Foreslope Hills, Fraser Delta, British Columbia, Canada. *Geo-Marine Letters*, 13, pp.219–226.

Hill, P.R. et al., 2008. Sedimentary processes and sediment dispersal in the southern Strait of Georgia, BC, Canada. *Marine Environmental Research*, 66(S), pp.S39–S48.

Hodgson, J.H. & Milne, W.G., 1951. Direction of Faulting in Certain Earthquakes of the North Pacific. *Bulletin of the Seismological Society of America*, 41, pp.221–242.
Ingledow, T. et al., 1957. British Columbia-Vancouver Island 138kV Submarine Power Cable. *The Institution of Electrical Engineers*, pp.1–15.

Johnson, S.Y., 1985. Eocene Strike-Slip Faulting and Nonmarine Basin Formation in Washignton. *Society of Economic Paleontologists and Minerologists*, pp.1–20.

Johnson, S.Y., 1991. Sedimentation and Tectonic Setting of the Chuckanut Formation, Northwest Washington. *Washington Geology*, 19, pp.12–13.

Johnson, S.Y., 1984. Stratigraphy, age, and paleogeography of the Eocene Chuckanut Formation, northwest Washington. *Canadian Journal of Earth Sciences*, 21, pp.92–109.

Johnson, S.Y. et al., 2004. Active shortening of the Cascadia forearc and implications for seismic hazards of the Puget Lowland. *Tectonics*, 23(1), p.TC1011.

Johnson, S.Y. et al., 1999. Active tectonics of the Seattle fault and central Puget Sound, Washington - Implications for earthquake hazards. *Geological Society of America Bulletin*, 111, pp.1042–1053.

Johnson, S.Y., Potter, C.J. & Armentrout, J.M., 1994. Origin and evolution of the Seattle fault and Seattle basin, Washington. *Geology*, 22, pp.71–74.

Johnson, S.Y., Potter, C.J., Armentrout, J.M., et al., 1996a. The southern Whidbey Island fault: An active structure in the Puget Lowland, Washington. *Geological Society of America Bulletin*, 108, pp.334–354.

Johnson, S.Y., Potter, C.J., Miller, J.J., et al., 1996b. The southern Whidbey Island fault: An active structure in the Puget Lowland, Washington. *Geological Society of America Bulletin*, 108(3), pp.334–354.

Johnson, S.Y., 1991. Sedimentation and Tectonic Setting of the Chuckanut Formation, Northwest Washington. *Washington Geology*, 19, pp.12–13.

Johnston, S.T. & Acton, S., 2003. The Eocene Southern Vancouver Island Orocline — a response to seamount accretion and the cause of fold-and-thrust belt and extensional basin formation. *Tectonophysics*, 365(1-4), pp.165–183.

Journeay, J.M. & Friedman, R.M., 1993. The coast belt thrust system: evidence if late Cretaceous shortening in southwester British Columbia. *Tectonics*, 12(3), pp.756–775.

Luternauer, J.L. et al., 1994. Fraser River delta: geology, geohazards and human impact J. W. H. Monger, ed. *Geological Survey of Canada Bulletin*, 481, pp.197–220.

Malone, S. D., R. S. Crosson, and A. I. Qamar (1997). Pacific Northwest seismograph network operations, 1997 Annual Report 1434-95-A- 1302, University of Washington, Seattle, Washington.

Mazzotti, S. et al., 2011. Seismic hazard in western Canada from GPS strain rates versus earthquake catalog. *Journal of Geophysical Research*, 116(B12), p.B12310.

Mazzotti, S.P. et al., 2002. GPS deformation in a region of high crustal seismicity: N. Cascadia forearc. *Earth and Planetary Science Letters*, 198, pp.41–48.

McCaffrey, R. & Goldfinger, C., 1995. Forearc Deformation and Great Subduction Earthquakes: Implications for STOR Cascadia Offshore Earthquake Potential. *Science*, 267, pp.856–859.

McCaffrey, R. et al., 2012. Active Tectonics of Northwestern US inferred from GPS-derived Surface Velocities. *Journal of Geophysical Research*.

McCaffrey, R. et al., 2000. Rotation and plate locking at the southern Cascadia subduction zone. *Geophysical Research Letters*, 27, pp.3117–3120.

McCrory, P.A. et al., 2012. Juan de Fuca slab geometry and its relation to Wadati-Benioff zone seismicity. *Journal of Geophysical Research*, 117(B9), p.B09306.

McKenna, G.T., Luternauer, J.L. & Kostaschuk, R.A., 1992. Large-scale mass wasting events on the Fraser River delta front near Sand Heads, British Columbia. *Canadian Geotechnical Journal*, 29, pp.151–156.

Mosher, D.C. & Thomson, R.E., 2002. The Foreslope Hills: large-scale, fine-grained sediment waves in the Strait of Georgia, British Columbia. *Marine Geology*, 192, pp.275–295.

Mosher, D.C. et al., 2000. Neotectonics in the Strait of Georgia: first tentative correlation of seismicity with shallow geologic structure in southwestern British Columbia. *Current Research*, 2000-A22, pp.1–11.

Mustard, P.S., 1991. Stratigraphy and Sedimentology of the Georgia Basin, British Columbia and Washington State. *Washington Geology*, 19, pp.7–9.

Mustard, P.S., 1994. The Upper Cretaceous Nanaimo Group, Georgia Basin J. W. H. Monger, ed. *Geological Survey of Canada Bulletin*, 481, pp.27–96.

Mustard, P.S. & Rouse, G.E., 1994. Stratigraphy and evolution of Tertiary Georgia Basin and subjacent Upper Cretaceous sedimentary rocks, southwestern British Columbia J. W. H. Monger, ed. *Geological Survey of Canada Bulletin*, 481, pp.97–170.

Petersen, M.D. et al., 2008. *Documentation for the 2008 Update of the United States National Seismic Hazard Maps*, U.S.G.S.

Rabinovich, A.B. et al., 2003. Numerical Modelling of Tsunamis Generated by Hypothetical Landslides in the Strait of Georgia, British Columbia. *Pure and Applied Geophysics*, 160, pp.1273–1313.

Riedel, M., 2002. *Report on Cruise PGC02002 on C.G.G. J.P. Tully*, Geological Survye of Canada.

Rogers, G.C. & Hasegawa, H.S., 1978. A Second Look at the British Columbia Earthquake of June 23, 1946. *Bulletin of the Seismological Society of America*, 68, pp.653–675.

Rusmore, M.E., Woodsworth, G.J. & Gehrels, G.E., 2000. Late Cretaceous evolution of the eastern Coast Mountains, Bella Coola, British Columbia. *Geological Society of America Special Paper 343*, pp.89–103.

Shaw, J.H. et al., 2005. *Seismic interpretation of contractional fault-related folds: an AAPG seismic atlas*, American Association of Petrolium Geologists.

Sherrod, B.L. et al., 2008. Finding concealed active faults: Extending the southern Whidbey Island fault across the Puget Lowland, Washington. *Journal of Geophysical Research*, 113(B5), p.B05313.

Suppe, J. & Medwedeff, D.A., 1990. Geometry and kinematics of fault-propagation folding. *Eclogae Geologicae Helvetiae*, 83(3), pp.409–454.

Tiffin, D.L., 1969. *Continuous Seismic Reflection Profiling in the Strait of Georgia, British Columbia*. University of British Columbia, unpublished PhD dissertation.

Thomas L Pratt, S.J.C.P.W.S.C.F., 1997. Seismic reflection images beneath Puget Sound, western Washington State: The Puget Lowland thrust sheet hypothesis. *Journal of Geophysical Research*, 102, pp.27–469–27–489.

Wells, R.E. & Heller, P.L., 1988. The relative contribution of accretion, shear, and extension to Cenozoic tectonic rotation in the Pacific Northwest. *Geological Society of America Bulletin*, 100, pp.325–338.

Wells, R.E. et al., 2003. Basin-centered asperities in great subduction zone earthquakes: A link between slip, subsidence, and subduction erosion? *Journal of Geophysical Research*, 108(B10).

Wells, R.E., Weaver, C.S. & Blakely, R.J., 1998. Fore-arc migration in Cascadia and its neotectonic significance. *Geology*, 26, pp.759–762.

Zelt, B.C. et al., 2001. Three-dimensional crustal velocity structure beneath the Strait of Georgia, British Columbia. *Geophysical Journal International*, 144, pp.695–712.

APPENDIX A. INVENTORY OF DIGITAL 2002 SHIPS SINGLE CHANNEL AIRGUN DATA

Line Name	# of Shots	Line Length [m]	meters/shot
Line_02	827	10920.20954	13.20460646
Line_03	1956	28003.50013	14.31671786
Line_04	754	10314.73605	13.68002129
Line_05	640	7535.070679	11.77354794
Line_06	732	6910.215236	9.440184749
Line_07a	408	2486.593883	6.09459285
Line_07b	1913	23028.73693	12.03802244
Line_08	83	1458.90422	17.57715928
Line_09	356	5958.100941	16.7362386
Line_10b	95	814.405136	8.572685642
Line_11	780	9801.348569	12.5658315
Line_12	765	10658.14848	13.93222024
Line_13	2939	38106.46728	12.96579356
Line_14	52	674.556772	12.97224562
Line_15b	94	1174.065365	12.49005707
Line_16	432	5071.485262	11.73954922
Line_17	741	13756.2836	12.52849144
Line_18	880	14869.31062	16.89694389
Line_19	621	10539.30211	16.97150098
Line_20	409	6920.586468	16.92074931
Line_21	465	7716.671171	16.59499177
Line_22a	152	1865.405634	12.27240549
Line_22b	1977	27735.3996	14.02903369
Line_23a	603	6561.027048	10.88064187
Line_23b	87	1097.080288	12.61011825
Line_24a	703	11080.42212	15.76162464
Line_24b	1707	23251.21503	13.62109844
Line_25	529	7119.596077	13.45859372
Line_26a	3906	57003.93817	14.59394218
Line_26b	130	1950.148687	15.00114375
Line_27	1721	19729.95401	11.46423824
Line_28	1406	20185.47984	14.35667129
Line_29	415	6441.815998	15.52244819
Line_30	237	2898.351565	12.2293315
Line_31	334	6111.13586	18.29681395
Line_32	788	10674.73001	13.54661169

Line Name	# of Shots	Line Length [m]	meters/shot
Line_33	723	7491.941242	10.36229771
Line_34a	89	1183.476617	13.29749008
Line_35	845	10080.57009	11.92966875
Line_36a	126	1712.474295	13.59106583
Line_36b	176	2397.963105	13.62479037
Line_36c	488	6945.321457	14.2322161
Line_37a	245	2453.344051	10.01364919
Line_37b	456	5992.989378	13.14252057
Line_38	803	2602.58997	3.2410834
Line_41	75	974.42486	12.99233147
Line_42	639	9144.489793	14.31062565
Line_43	116	1437.026069	12.38815577
Line_44	741	9499.088076	12.81928215
Line_45a	53	680.827834	12.84580819
Line_45b	751	10129.76361	13.48836699
Line_46a	94	1204.708284	12.81604557
Line_46b	798	9401.442861	11.78125672
Line_47	51	723.981406	14.19571384
Line_49a	343	3230.581714	9.41860558
Line_49a1	343	3243.97446	9.457651487
Line_49b	114	1238.486646	10.86391795
Line_49c	942	11697.14745	12.41735398
Line_50	134	1968.177067	14.68788856
Line_51	1211	17068.95393	14.0949248
Line_52a	108	1569.22986	14.52990611
Line_52b	283	4371.326988	15.44638512
Line_52c	82	1162.933535	14.18211628
Line_53b	502	7571.325159	15.08232103
Line_54a	81	1460.797935	18.03454241
Line_54b	1442	20356.23358	14.11666684
Line_55a	266	3523.488481	13.2461973
Line_55b	89	1352.658027	15.1984048
Line_55c	1432	19184.10892	13.39672411
Line_56	1603	20189.83989	12.59503424
Line_57	1400	19738.4346	14.09888186
Line_58	241	2944.392869	12.2173978
Line_59	1329	18075.29937	13.60067673
Line_60_62	507	10069.78456	19.86150801
Line_60a	333	4209.461693	12.64102611
Line_60b	1203	17645.43882	14.66786269

Line Name	# of Shots	Line Length [m]	meters/shot
Line_61	1490	18756.22154	12.58806815
Line_62a	252	3365.113297	13.35362419
Line_62b	1569	19258.48885	12.27437148
Line_63a	238	3576.996561	15.02939732
Line_63b	1206	17762.49082	14.72843352
Line_64a	74	1129.386527	15.26198009
Line_64b	1249	16691.9206	13.36422786
Line_65	1482	17968.56641	12.12453874
Line_66	1110	18132.53588	16.33561791
Line_66b	99	1071.434275	10.82256843
Line_67	9	101.726572	11.30295244
Line_68a	111	1232.223751	11.10111487
Line_68b	883	11201.08786	12.68526371
Line_69	924	12289.55406	13.30038318
Line_70a	111	1602.406261	14.43609244
Line_70b	950	14255.2646	15.00554168
Line_71a	16	200.060502	12.50378138
Line_72a	133	1724.356783	12.96508859
Line_72b	1338	16387.27813	12.24759203
Line_73a	66	806.852965	12.22504492
Line_73b	1432	17680.79301	12.34692249
Line_74a	132	1892.846427	14.33974566
Line_74b	950	13875.25677	14.60553344
Line_75	853	11360.93349	13.31879659

APPENDIX B. TIF2SEGY CONVERSIONS

Airgun data for Lines 8 and 10 was not collected digitally in SEGY format. It is not entirely clear what happened but the cruise report notes the COAMS system experienced a series of short circuits and system failures during this early portion of the cruise. It's presumed these issues impacted the Teledyne system in one way or another and resulted in no digital data for Lines 8 and 10. Both Lines 8 and 10 were recorded on paper RefTek systems, these paper copies were then scanned and converted to SEGY data files using the shell script tif2segy created by Andrew McRae. These data files are not true SEGY data but simply the images written in the SEGY format so they could be displayed by seismic software thus these files cannot be processed as SEGY data, e.g. migrated.

Below is a table listing the start and end times of digitally collected lines and time-points written on paper RefTek versions of Lines 8 and 10. Times indicate significant overlap of lines. The following is a proposed scenario explain this overlap:

- Line 7 was recorded longer than planned
- Line 8 was not recorded digitally but the paper RefTek copies were marked for the planned Line 8
- Since Line 8 was not being digitally recorded, Line 9 recording started early; the early part of Line 9 was planned to be the end of Line 8 thus the paper copy records the early part of the digital Line 9 as the end of Line 8
- Similarly, the digital recording of Line 9 went longer than planned and the paper copy indicates the start of Line 10.

Paper copies of Lines 7 and 9 would be needed to verify this.

Line	start time [d:h:m:s]	end time [d:h:m:s]
7	135:18:12:53	135:21:07:56

	time point [h:m:s]	trace number
8	21:00:23	96
	21:30:22	965
	22:00:21	1942
	22:30:21	2915
	23:00:20	3891

	start time [d:h:m:s]	end time [d:h:m:s]
9	135:22:51:15	135:23:23:45

	time point [h:m:s]	trace number
10	23:00:20	290
	23:30:19	1300
	0:29:59	3240

	start time [d:h:m:s]	end time [d:h:m:s]
11	136:07:46:48	136:08:51:42

APPENDIX C. FIGURES

1. General Geology & Data Sets

Bounded by Vancouver Island to the west, mainland North America to the east, and the San Juan Islands to the south, the Strait of Georgia is a local depression in the Cascadia forearc filled with Cretaceous and Eocene strata. Index map shows Cascadia Subduction Zone resulting from the Pacific plate subducting beneath North America as red line with teeth on subducting Pacific Plate. Gulf Islands are outlined with grey, San Juan Islands with white, all other coastlines are black; Satuma Island (SI), Tombo Island (TI). Bolder black line indicates section displayed in figure 2.

2. SHIPS 1998 bare & interpreted

See figure 1 for location.

a) Un-interpreted section

b) Interpreted section

The southern portion of Nanaimo Basin appears to be deformed by two trust systems, one northwest verging and one southeast verging. “Secondary faults” of the Cowichan Fold and Thrust belt mapped by England (1989) and breaks between Gulf Islands project northeast to fold axial surfaces observed in profile. Proximity to the San Juan Islands suggests the southern thrust system is in fact the northern continuation of the San Juan Thrust System; there is no previously identified thrust system to correlate the northern folds with. A narrow --- meter window exists between the Eocene surface of Tumbo Island and the Cretaceous surface of Saturna Island a series of parallel bedrock ridges constrain the K-E boundary to this window along the Gulf Islands. A bedrock ridge continues north from Tumbo Island to intersect with the seismic profile and provide stratigraphic control. Growth strata beds are highlighted in blue, possible on-lapping strata in cyan. P-nodal (Cassidy et al, 2000) solutions plotted; M_L 4.6 mainshock (278,56,120) and M_L 3.4 foreshock (236,42,123) figure 4 displays Cassidy’s earthquake relocations for the 1997 M_L 4.6.

3. Fault system strike

Kinks the in the bathymetric bedrock ridge defining the Cretaceous-Eocene boundary project northeast (black dashed lines) to fold hinges on the seismic section, establishing trends for faults observed in section; faults appear to be offshore continuations of England’s (1989) “secondary faults” noted to be younger than the Cowichan Fold and Thrust Belt. Dashed red lines project faults near 1997 earthquake (figure 5) onto the map using same general strike. See figure 7 for legend. (Note that true fault strike is slightly more east than depicted by black dashed lines due to the offset of the seismic section from the mapped track line.)

4. 1997 Earthquake

a) un-interpreted section with earthquake relocations.

Between stations 7800 and 8200 reflector coherency is lost in narrow vertical zones and several reflectors have abrupt angular changes, these trace up to the bedrock surface as reflector terminations. Vertical exaggeration of ~2.

b) Interpreted section with focal mechanism

Relocated focal mechanism solutions for the M_L 4.6 mainshock and M_L 3.4 foreshock (Cassidy et al) are plotted. Apparent bedrock surface displacements and abrupt reflector angle changes are

interpreted as a group of shallow splay faults from a north dipping listric thrust fault. Note angle of focal mechanism does not agree with the interpreted fault due to vertical exaggeration of 2.

c) 2002 SHIPS; Line 61 subsection; Teledyne

Sediments show localized deformation in the regions around stations 500, 700, and 950. Sediment at station 700 is displaced as a 250m deep by 800m wide triangular package. Sediment reflectors become transparent at station 950 and continue north suggesting gas hydrates.

d) 2002 SHIPS; Line 64b subsection; Teledyne

Sediments are displaced in three triangular packages between stations 950 and 750. Connecting the largest package and the one on Line 61 has a trend of 10 degrees north of east, passing over the relocated earthquakes and interpreted thrust fault.

5. Sandy Point structures

(a) Location map showing lines from Western Geophysical & Centennial cruises; bold lines indicate portion of line shown.

(b) Western Geophysical line W2

(c) Western Geophysical line W3

Both lines trend north-south and are dominated by a ~2.5 km thick sedimentary sequence. Strikes proposed by Kelsey et al for Sandy Point Fault project to these terminations; the inflection point in reflectors at the north end of W3 is correlated with the Birch Bay Fault. Stratigraphic control is established by correlating reflector packages with industry line AHEL 1 (Hurst 1991); line AHEL 1 has stratigraphic control from dating preformed on the industry well AHEL (Hurst 1991). Geologic units of the San Juans are carries off-shore via high-resolution bathymetry to interpret reflectors south of the Sandy Point Fault. South of the Sandy Point Fault reflector coherence is lost at shallow depths despite sedimentary near the surface; loss of reflectors could be due to: change in lithology without a strong interface reflector, contact metamorphism due to igneous intrusions, or rapid source attenuation due to a zone of highly faulted material (Lummi Island Tectonic Zone, WA state geologic map) Sense of motion proposed by Kelsey et al (2012) on Sandy Point and Birch Bay Faults are shown with large back arrows above each section. White lines demark multiples.

(d) Western Geophysical line W4:

(e) Centennial line SJ1:

(f) Zoom of Centennial line SJ1 above updip projection of Sandy Point Fault.

(g) Centennial line SJ2: Orange line demarks angular unconformity within Quaternary deposits.

(h) Zoom of Centennial line SJ2 above updip projection of Sandy Point Fault

Both lines trend north-south and are dominated by a ~2.5 km thick sedimentary sequence. Strikes proposed by Kelsey et al for Sandy Point Fault project to these terminations; the inflection point in reflectors at the north end of W3 is correlated with the Birch Bay Fault. Stratigraphic control is established by correlating reflector packages with industry line AHEL 1 (Hurst 1991); line AHEL 1 has stratigraphic control from dating preformed on the industry well AHEL (Hurst 1991). Geologic units of the San Juans are carries off-shore via high-resolution bathymetry to interpret reflectors south of the Sandy Point Fault. South of the Sandy Point Fault reflector coherence is lost at shallow depths despite sedimentary near the surface; loss of reflectors could

be due to: change in lithology without a strong interface reflector, contact metamorphism due to igneous intrusions, or rapid source attenuation due to a zone of highly faulted material.

6. Outer Island Fault Review.

a) Tomography slices from Dash et al 2007. Dashed red box on N2 indicates approximate area imaged by Tiffin (1969) with 5000 joule multichannel sparker.
b) Multichannel sparker lines collected by Tiffin in 1969 show folded strata above Dash et al's (2007) proposed location of the Outer Island Fault. Reflectors dipping steeply to the east are consistent England's observations (1991,1998).

7. Geologic Map

Notable updates include, defining the Cretaceous-Eocene boundary, extending Sandy Point structures further northwest, identification of the Border Fault and North San Juans Block, identifying an active fault in the region of the 1997 earthquake, redefining and extending England's 'secondary faults', and Dash's proposed blind thrust interpretation of the Outer Island Fault supported by folded strata observed on Tiffin's (1969) sparker lines.

8. Schematic of Cretaceous to present deformation of the Georgia Basin

a) South dipping basin with east-northeast approaching San Juan Terrane.
b) Terrane (not pictured) impacts basin causing minor north-south folding and large east-west shortening initiating a ramp and flat geometry. Here the nose of the hanging wall is assumed to be brecciated erode during thrusting.
c) Final configuration with duplexed strata forming a new higher eastern bank for the basin.

9. Progression of tectonic theory for Georgia Basin, see text for discussion. Modified from Mustard 1994.

Insular Belt

Cretaceous strata

Wrangellia Terrane

Eocene strata

Crescent Terrane

San Juan/ North Cascades Terrane

Nanaimo

Gabriola Island

Vancouver, B.C.

Point Roberts

Bellingham

Sucia Island

SI

TI

Orcas Island

San Juan Island

Sidney

Victoria

0 5 10 20 30 40 Kilometer

SHIPS 2002
SHIPS 1998
Centennial
Dash
Western Geo. Phys.
Tiffin

N

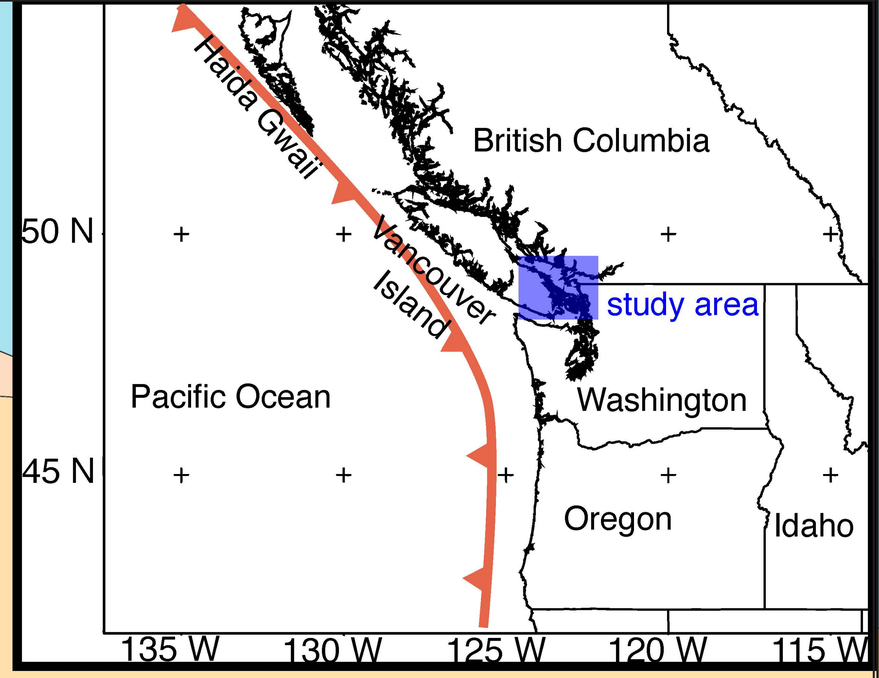

Cretaceous-Eocene *unconformity* length of 46.136km

v.e. 1:1

Linear distance of 46km

Northwest

distance along line (km)

Southeast

10 20 30 40 50 60 70 80 90 100

approximate depth (km)

0 1 2 3 4 5 6 7 8

Quaternary

Eocene

chaotic reflectors

Cretaceous

1km

10km

(ve: 4:1)

10°

40°

(b)

1997 Gabriola earthquake sequence

Vancouver Fold and Thrust Belt

San Juan Thrust System

(a)

Northwest

distance along line (km)

Southeast

10 20 30 40 50 60 70 80 90 100

0 1 2 3 4 5 6 7 8

approximate depth (km)

North

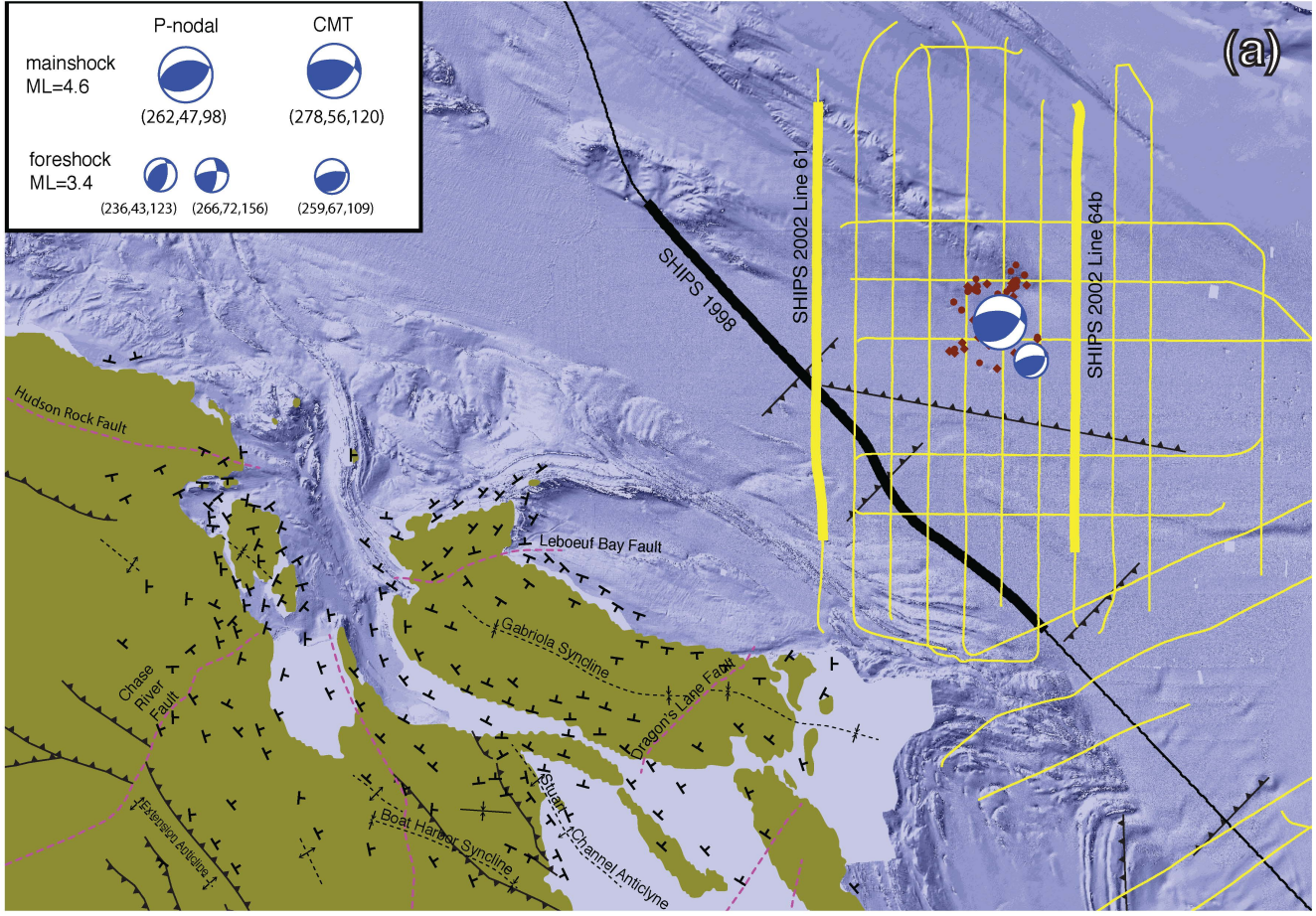

Section of SHIPS 1998 Line

Mosher et al, (2000)

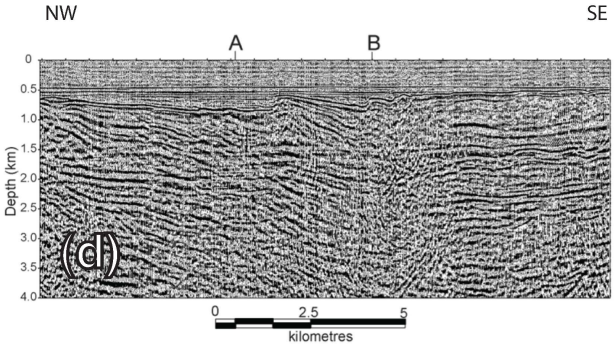

This Study

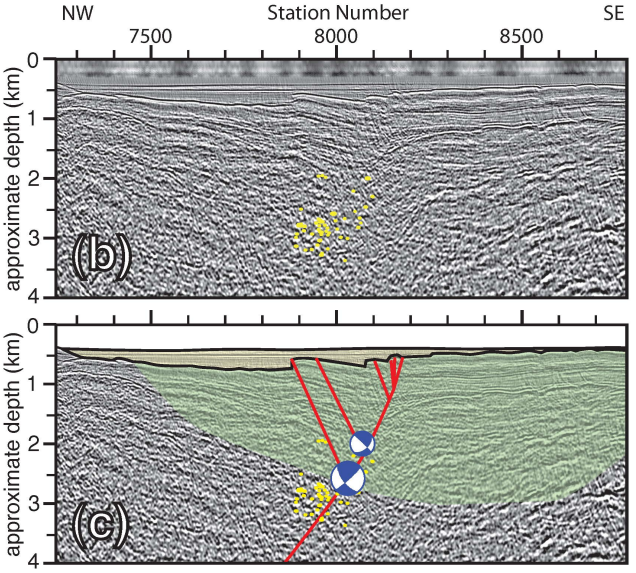

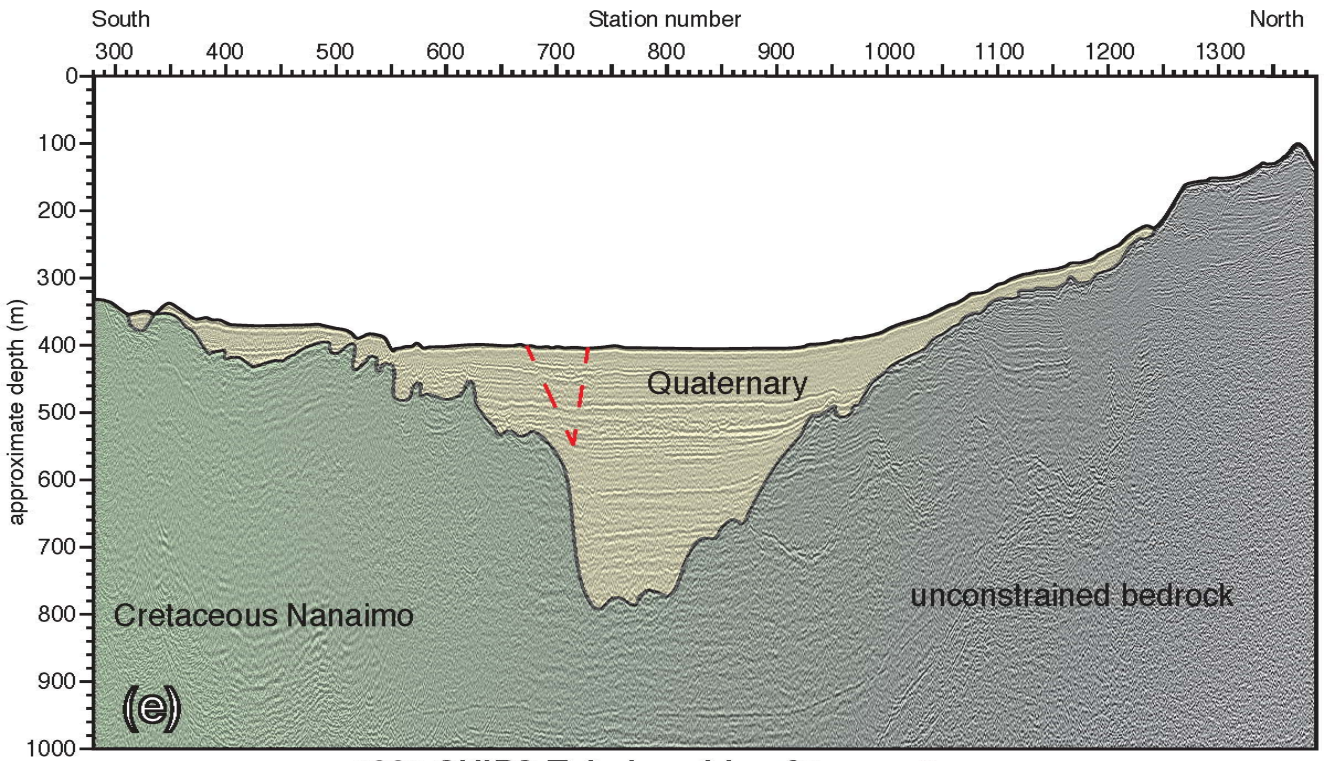

2002 SHIPS Teledyne Line 61 ve~8

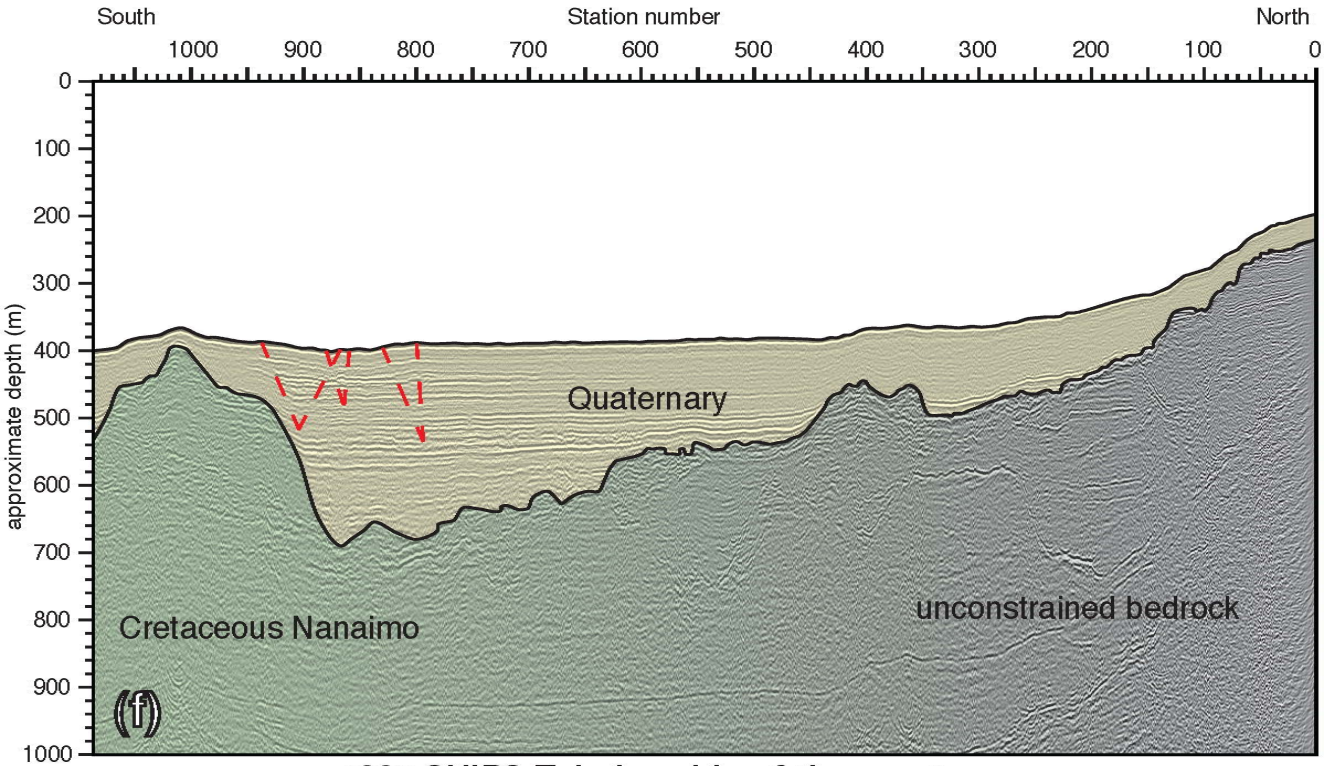

2002 SHIPS Teledyne Line 64b ve~8

(a)

Canada
United States

Point
Roberts

Drayton Harbor Fault

W4

W2

W3

?

?

Birch Bay Fault

?

?

Satuma
Island

Sucia Island

SJ2

SJ1

Sandy Point Fault

Bellingham

Lummi Island

Orcas
Island

Northwest

Western Geophysical: line W4
distance along line (km)

Line W2 crossing

Line W3 crossing

Fault?

Southeast

0

5

10

15

20

25

approximate depth below water surface (km) - vertical exaggeration ~2

1

2

3

4

5

6

(d)

South

Western Geophysical: line W2 - distance along line (km)

Line W4 crossing

North

0 5 10 15 20

approximate depth below water surface (km) - vertical exageration ~2

0 1 2 3 4 5 6

Kn

Ec

Sandy Point Fault

Eocene Chuckanut (Ec)

Cretaceous Nanaimo (Kn)

San Juan
Thrust System

(b)

Southeast

Western Geophysical: line W3 - distance along line (km)

Line W4 crossing

Northwest

0 5 10 15 20 25 30

approximate depth below water surface (km) - vertical exageration ~2

0 1 2 3 4 5 6

Kn

Ec

Kn

Ec

Sandy Point Fault

Eocene Chuckanut (Ec)

paraconformity

Birch Bay Fault

Cretaceous Nanaimo (Kn)

Detachment?

Cretaceous Nanaimo?

?

San Juan
Thrust System

intrusive
igneous?

(c)

Southwest

Centennial: Line SJ1 - distance along line (km)

Northeast

9 10 11

approximate depth below water surface (m) - vertical exageration ~8

10 20 30 40 50 60 70 80 90 100 110

Quaternary

multiple

multiple

(f)

Southwest

Centennial: line SJ1 - distance along line (km)

Expected Sandy Point Fault

Northeast

0 1 2 3 4 5 6 7 8 9 10 11 12 13

approximate depth below water surface (m) - vertical exageration ~8

100 200 300 400 500

Quaternary

Eocene

Quaternary

Eocene

Quaternary

multiple

multiple

multiple

multiple

multiple

multiple

multiple

multiple

multiple

multiple

multiple

(e)

Southwest

Centennial: Line SJ2 - distance along line (km)

Northeast

6

7

approximate depth below water surface (m) - vertical exageration ~8

50

60

70

80

90

100

110

120

130

140

150

multiple

(h)

Southwest

Centennial: Line SJ2 - distance along line (km)

Expected Sandy Point Fault

Northeast

0

1

2

3

4

5

6

7

8

9

approximate depth below water surface (m) - vertical exageration ~8

100

200

300

400

500

Quaternary

Eocene

multiple

multiple

multiple

multiple

multiple

multiple

multiple

multiple

multiple

(g)

Figure 7

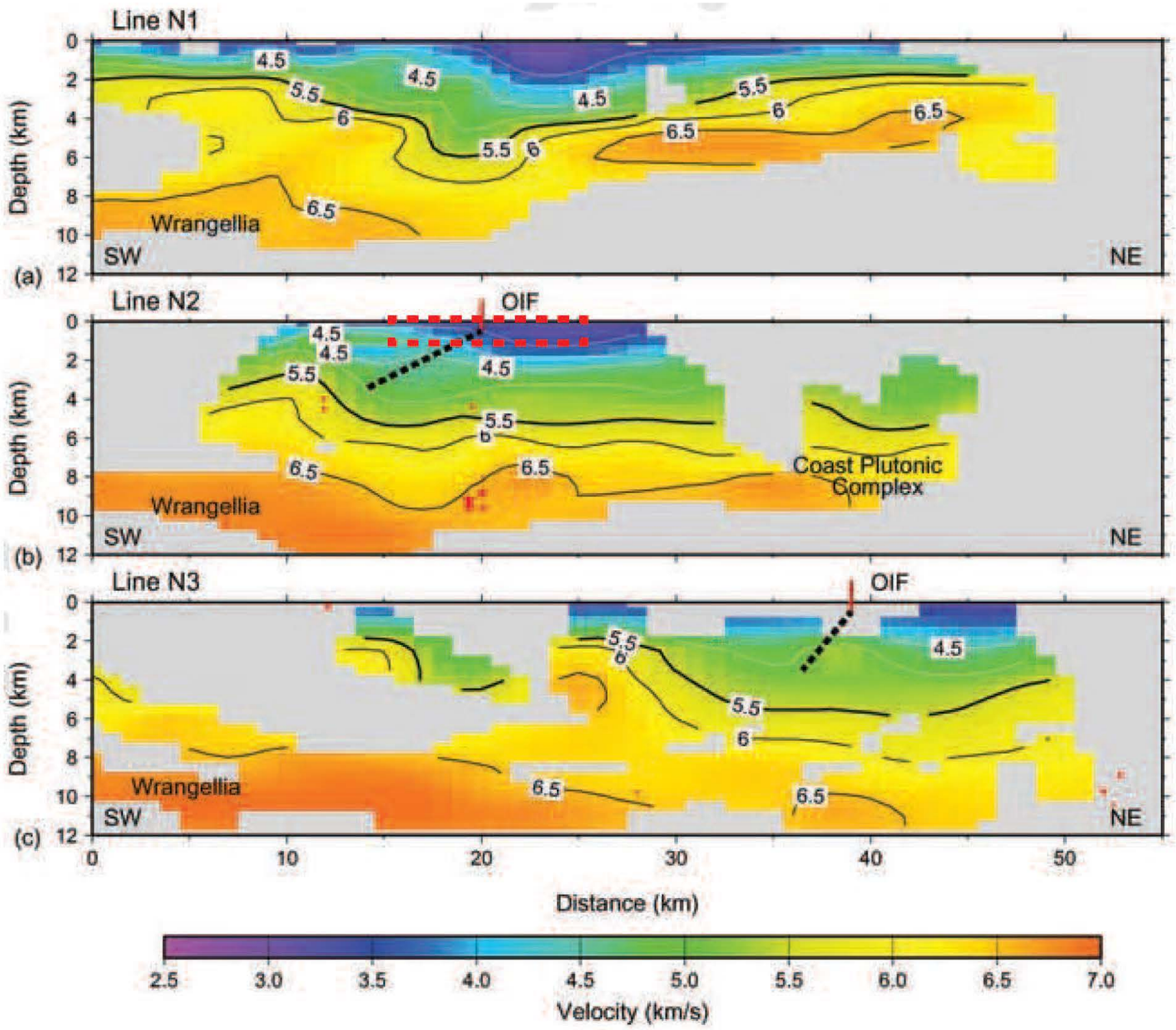
Line N1
Depth (km)
SW
NE
Wrangellia
(a)
Line N2
OIF
Coast Plutonic Complex
(b)
Line N3
(c)
Distance (km)
Velocity (km/s)

Tiffin Line 21
Length Along Line (km)
Approximate Depth (m)
Bedrock
Holocene
Pleistocene
Bedrock
Outer Island Fault

Tiffin Line 17
Length Along Line (km)
Approximate Depth (m)
Bedrock
Holocene
Bedrock
Bedrock
Pleistocene
Pleistocene
Outer Island Fault

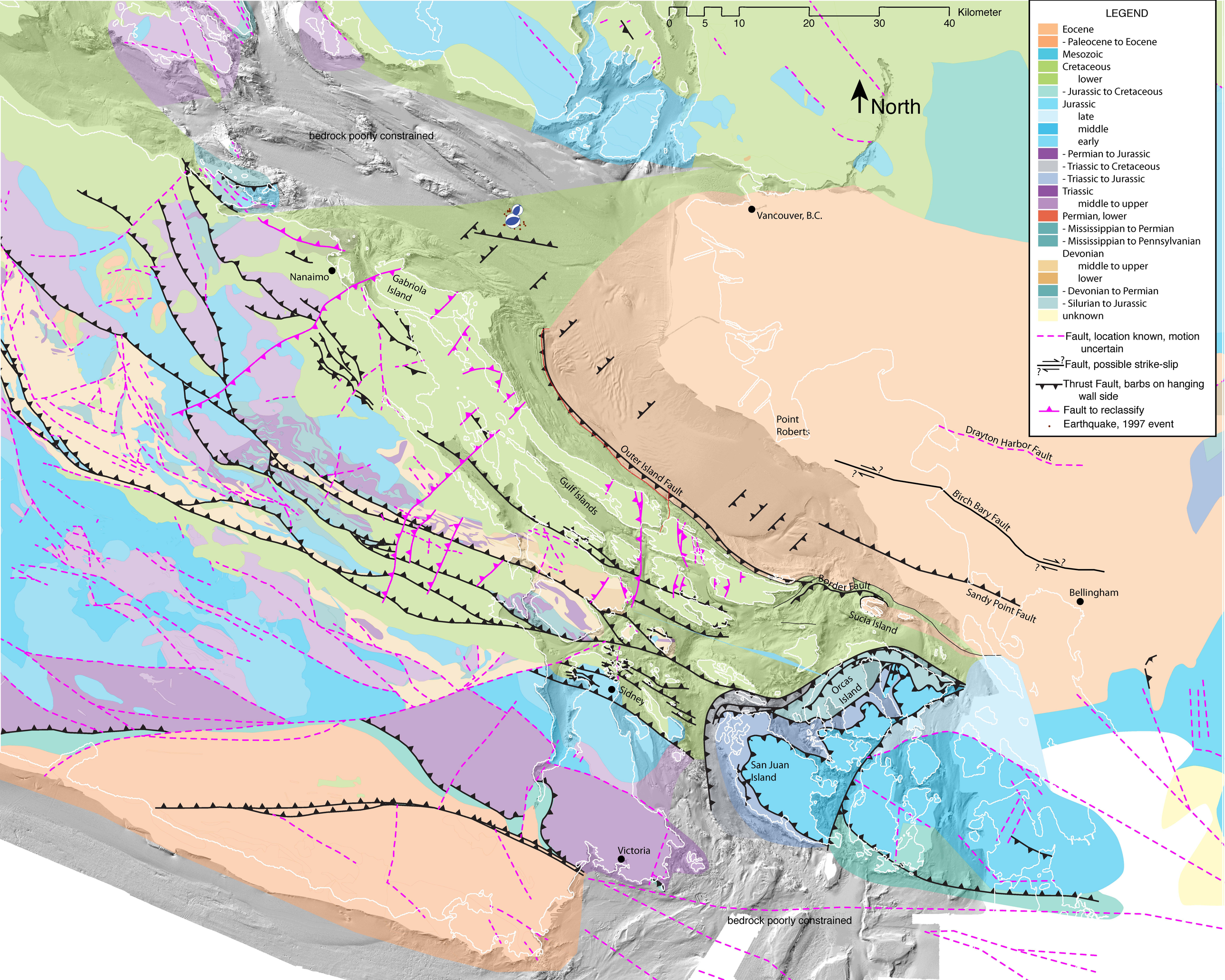
Kilometer
0
5
10
20
30
40
North
bedrock poorly constrained
Vancouver, B.C.
Nanaimo
Gabriola Island
Point Roberts
Drayton Harbor Fault
Outer Island Fault
Gulf Islands
Birch Bary Fault
Border Fault
Sucia Island
Sandy Point Fault
Bellingham
Sidney
Orcas Island
San Juan Island
Victoria
bedrock poorly constrained
LEGEND
Eocene
- Paleocene to Eocene
Mesozoic
Cretaceous
lower
- Jurassic to Cretaceous
Jurassic
late
middle
early
- Permian to Jurassic
- Triassic to Cretaceous
- Triassic to Jurassic
Triassic
middle to upper
Permian, lower
- Mississippian to Permian
- Mississippian to Pennsylvanian
Devonian
middle to upper
lower
- Devonian to Permian
- Silurian to Jurassic
unknown
Fault, location known, motion uncertain
Fault, possible strike-slip
Thrust Fault, barbs on hanging wall side
Fault to reclassify
Earthquake, 1997 event

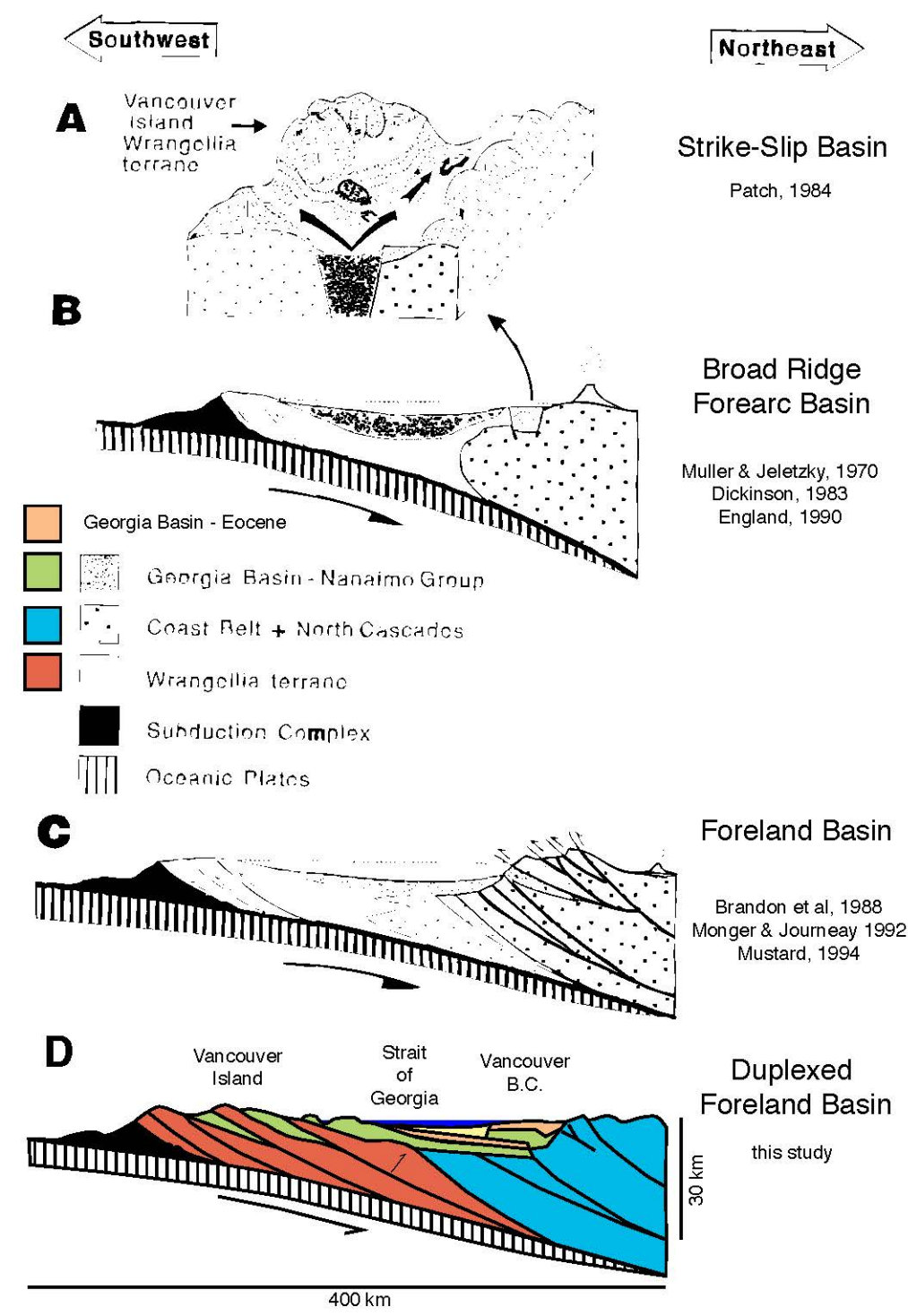

Modified from Mustard 1994

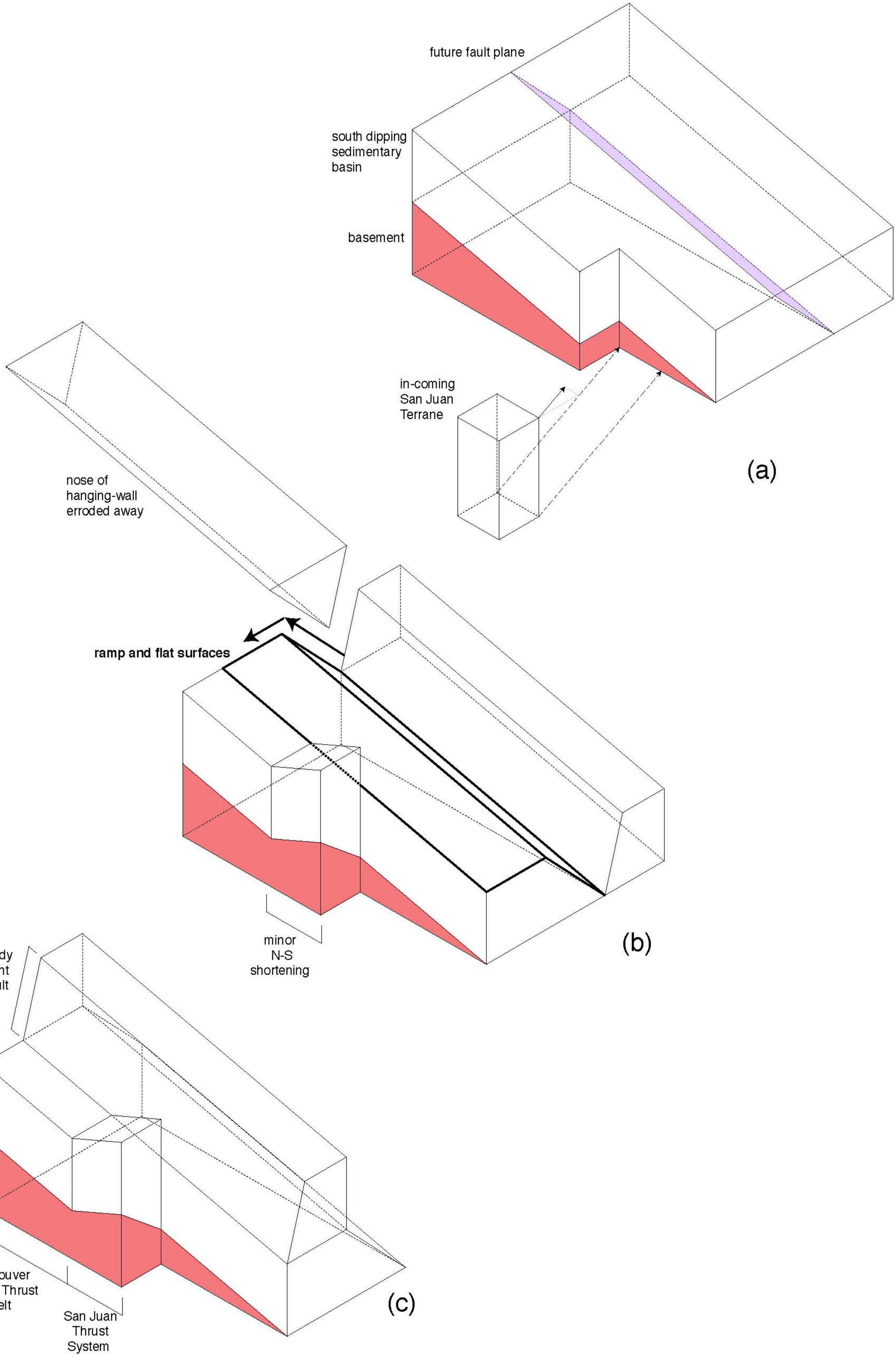
future fault plane
south dipping
sedimentary
basin
basement
in-coming
San Juan
Terrane
(a)
nose of
hanging-wall
erroded away
ramp and flat surfaces
minor
N-S
shortening
(b)
Sandy
Point
Fault
Vancouver
Fold & Thrust
Belt
San Juan
Thrust
System
(c)